Numerical Techniques for the Treatment of Quasistatic Solid Viscoelastic Stress Problems

S. Shaw
M.K. Warby
J.R. Whiteman
C. Dawson
M.F. Wheeler

January 1993

TR93-02

Numerical Techniques For The Treatment of Quasistatic Solid Viscoelastic Stress Problems.

S.Shaw†, M.K.Warby and J.R.Whiteman‡.
BICOM, *Institute of Computational Mathematics, Brunel University, Uxbridge, England.*

C.Dawson and M.F.Wheeler.
Department of Mathemetical Sciences, Rice University, Houston, U.S.A.

Abstract.

For quasistatic stress problems two alternative constitutive relationships expressing the stress in a linear viscoelastic solid body as a linear functional of the strain are derived. In conjunction with the equations of equilibrium, these form the mathematical models for the stress problems. These models are first discretized in the space domain using a finite element method and semi-discrete error estimates are presented corresponding to each constitutive relationship. Through the use respectively of quadrature rules and finite difference replacements each semi-discrete scheme is fully discretized into the time domain so that two practical algorithms suitable for the numerical stress analysis of linear viscoelastic solids are produced. The semi-discrete estimates are then also extended into the time domain to give spatially $\mathcal{H}^1$ error estimates for each algorithm.

The numerical schemes are predicated on exact analytical solutions for a simple model problem, and finally on design data for a real polymeric material.

1 Introduction.

1.1 Outline.

This paper is concerned with the computational modelling of problems of solid mechanics in which the material is assumed to be linear viscoelastic and the deformation is quasistatic (i.e. the inertia term in the momentum equations is neglected, providing equilibrium equations). For any problem of this type our purpose here is to produce a mathematical model, to discretize this to produce a numerical algorithm, to derive *a priori* error estimates for the error associated with the numerical solution and to apply the scheme to a number of test problems for numerical verification. We have additionally applied the algorithm to a problem involving experimental data from a specific polymeric material.

Two forms of the constitutive relation are proposed, giving two models. These involve the rate of change with time respectively of the *stress relaxation function* [1,3,4] and the *displacement vector*. Both models are first discretized in the space variables using a Galerkin technique, thus setting up semi-discrete approximating problems. These are further discretized in time through the application respectively of quadrature rules and finite difference replacements, thus producing two fully discrete approximating formulations. The errors in these are analysed and, in §§3,4, *a priori* estimates, for the semi-discrete and fully discrete schemes respectively, are derived. The results of numerical experiments are given in §5 for some problems where the exact solutions have been obtained through application of the correspondence principle of Schapery [3,4], and for the specific polymeric material as above.

1.2 Viscoelastic materials.

The stress analysis of solid materials is usually restricted to the cases either of *linear elasticity*, under the assumptions that the deflections considered are in some sense small and that the stresses occuring in the body never exceed the yield stress of the material, or of *plasticity* where the yield stress is exceeded and some permanent deformation of the material takes place. Whereas linear elasticity utilises a simple relationship (Hooke's law) between stress and strain, plasticity is a nonlinear phenomena and in *flow* theory the constitutive relationship is strain rate dependent and thus depends on the loading history.

† Supported by an SERC studentship.

‡ Supported in part by the United States Army Research and Standardization Group, Europe, under contract No. DAJA45-89-C-003

There is, however, a class of materials, solids and fluids, the deformation of which can be modelled using linear theory, but for which linear elasticity is not appropriate. These materials are termed *viscoelastic* since in deformation they display both elastic and viscous flow properties.

Perhaps the most common examples of viscoelastic materials in engineering science are the thermoplastic polymers. In simple terms such materials may be considered to be composed of many so called long chain molecules arranged more or less at random and intertwining with each other in a "spaghetti" like manner. Neighbouring chains may be joined to each other by *cross-linking*. When a mechanical load is applied to such a material there will be an *elastic deflection*, due to the the ability of each chain to stretch, and a *viscous flow*, caused by the sliding of the molecules over one another; the extent to which molecules may slide in this way is determined by the amount of cross-linking. This dual (elastic plus viscous) effect gives rise to the term *viscoelasticity*. If the degree of cross-linking is very small the flow may continue unchecked and the material is considered to be a viscoelastic liquid. Conversely, if the degree is high the flow will eventually cease (unless the applied load is large enough to rupture the material) and the material is a viscoelastic solid. In practice this distinction may be somewhat blurred, particularly in nonisothermal contexts near the melt temperatures of viscoelastic materials.

In the present paper we consider only compressible, isotropic viscoelastic media undergoing "small" deformations subject to isothermal, quasistatic conditions.

1.3 Linear viscoelasticity.

Experimental observations of viscoelastic materials under loads, see e.g. [3], suggest that at any given time the stress at a point in a viscoelastic medium depends not only on the current strain at that point but upon the entire strain history from the instant that the material was in its original unstressed state. For this reason viscoelastic materials are described as having *memory*. Mathematically this suggests that the stress may be written as a functional of the strain, or *vice-versa*; a linear functional gives rise to the linear viscoelastic model. When the material function involved in this functional depends only upon the relative time (i.e. the algebraic difference between the present time and the time in the deformation or loading history) the material so described is termed "non-ageing".

In order to arrive at an explicit representation of this functional we have the following:

Hypothesis 1.3.1. The Boltzmann superposition principle [4].

For a linear, non-ageing viscoelastic body the stress arising at position x and time t from a sequence of strain increments $\{\Delta\varepsilon(x,t_i)\}_{i=0}^{N-1}$, $t_{N-1} < t$, applied to the body may be expressed as the sum of the stresses $\{\Delta\sigma^i(x,t)\}_{i=0}^{N-1}$ induced by each individual strain increment.

Two readily observable phenomena characterizing a viscoelastic material are those of *creep* and *stress relaxation*. Consider a slim viscoelastic cylindrical bar subjected to a constant axial (tensile) load. In the deformation one would observe an instantaneous elastic deflection followed by a viscous flow, possibly up to some equilibrium deformation; this is termed creep. Now, consider a similar bar subjected to a constant axial strain. The stress in the bar will instantaneously increase as an elastic response and will thereafter decay to some constant (possibly zero) value; this is stress relaxation.

2 Governing equations.

2.1 Constitutive relationship.

For every time $t \in \mathcal{I} := [0,t_I]$ we consider the deformation of an isotropic viscoelastic body $\mathcal{G}$, characteristically solid, the interior of which occupies the region $\Omega \subset \mathcal{R}^n$, where $n = 2,3$, with convex polygonal or polyhedral boundary $\partial\Omega$ and resisting the action of a body force $f := (f_i)_{i=1}^n$ and a surface traction $g := (g_i)_{i=1}^n$. The resulting displacement at a point $x := (x_i)_{i=1}^n \in \overline{\Omega} := \Omega \bigcup \partial\Omega$, the reference configuration, is denoted by $u := (u_i)_{i=1}^n$, and the components of the symmetric stress and strain tensors are denoted, respectively, by σ_{ij} and ε_{ij}, where $1 \le i,j \le n$. For the purposes of calculation these components will be ordered in $\frac{1}{2}n(n+1)$-tuplets, such that, for $n = 3$:-

$$\sigma := (\sigma_{11}\ \sigma_{22}\ \sigma_{33}\ \sigma_{12}\ \sigma_{13}\ \sigma_{23})^T, \tag{2.1.1}$$

$$\varepsilon := (\varepsilon_{11}\ \varepsilon_{22}\ \varepsilon_{33}\ \varepsilon_{12}\ \varepsilon_{13}\ \varepsilon_{23})^T. \tag{2.1.2}$$

with the reduction to lower space dimensions being obvious. It is to be understood that $(w_i)_{i=1}^n$ symbolises an ordered n-tuplet, $(w_1, \ldots, w_n)^T \in \mathcal{D}^n$, where $\mathcal{D}$ is some appropriate set containing the w_i. The strain tensor is obtained from the displacements via

$$\varepsilon_{ij} := \frac{1}{2}\left(\frac{\partial u_i}{\partial x_j} + \frac{\partial u_j}{\partial x_i}\right). \tag{2.1.3}$$

In isotropic linear elasticity there is a constitutive relationship between stress and strain given by Hooke's law. In component form this relation can be expressed as

$$\sigma_{ij}(x) = \lambda(x)\nabla\cdot u(x)\delta_{ij} + \mu(x)\varepsilon_{ij}(u(x)), \qquad (2.1.4)_1$$

or equivalently in vector-matrix notation the law can be expressed as

$$\sigma(x) = D(x)\varepsilon(x), \qquad (2.1.4)_2$$

where λ and μ are the Lamé coefficients, δ_{ij} is the Kronecker delta, $\nabla\cdot$ is the divergence operator and D is the constitutive matrix. From $(2.1.4)_1$ and $(2.1.4)_2$ if follows that the elements of D are given in terms of λ and μ. Thus for a general compressible linear elastic material, the constitutive relation involves two independent scalar functions of position which, as is given above, can be taken as λ and μ. These may be the best pair of functions to take for the mathematical neatness of equations $(2.1.4)_1$ but other functions are often more useful in describing the physical features of a deformation. Specifically we have the bulk modulus K, Young's modulus E, the shear modulus G and Poisson's ratio ν which are given respectively by

$$K = \lambda + \frac{1}{3}\mu, \quad E = \frac{G(3\lambda + 2G)}{\lambda + G}, \quad G = \mu/2 \quad \text{and} \quad \nu = \frac{\lambda}{2(\lambda + G)} \tag{2.1.5}$$

and for most elastic materials we would expect

$$K > 0, \quad E > 0 \quad \text{and} \quad \mu > 0 \tag{2.1.6}$$

which implies that $-1 < \nu < 0.5$ but in general we would expect that $0 < \nu < 0.5$ which corresponds to $\lambda > 0$.

In order to arrive at a constitutive relationship linking stress and strain for a linear viscoelastic material at a particular time t we use hypothesis 1.3.1 in conjunction with a Hooke's law type relation. We do this as follows. We let $x \in \Omega$ be a fixed point and we suppose that the strain history at x is of the form shown in Fig. 2.1.1. That is we suppose that each component of strain is a step function with respect to the times $t_0 < t_1 < \ldots < t_{N-1}$. Specifically we have

$$\varepsilon(x,t) = \begin{cases} 0, & t < t_0, \\ \varepsilon^i(x), & t_i < t < t_{i+1}, \quad i = 0, 1, \ldots, N-1 \ . \end{cases} \tag{2.1.7}$$

and thus the corresponding strain increments $\Delta\varepsilon(x, t_i)$ are given by

$$\Delta\varepsilon(x,t_i) = \begin{cases} \varepsilon^0(x), & i = 0 \\ \varepsilon^i(x) - \varepsilon^{i-1}(x), & 1 \le i \le N-1 \ . \end{cases} \tag{2.1.8}$$

The first strain increment $\Delta\varepsilon(x, t_0) = \varepsilon^0(x)$ gives rise to a stress $\sigma^0(x,t)$ which in the case of a viscoelastic material decays the further the time t is from the time t_0 when the increment was applied. That is mathematically we have

$$\sigma^0(x,t) = D(x, t - t_0)\varepsilon(x, t_0), \quad t \ge t_0, \tag{2.1.9}$$

where the matrix function D in Hooke's law, which only depends on position, is now replaced by the matrix function D which depends both on position and the elapsed time with the components of D decreasing monotonically with the elapsed time. In (2.1.9), $\sigma^0(x,t)$ is of course also the stress increment $\Delta\sigma^0(x,t)$. Similarly the stress increment corresponding to the strain increment $\Delta\varepsilon(x,t_i)$ is given

$$\Delta\sigma^i(x,t) = D(x, t - t_i)\Delta\varepsilon(x, t_i), \quad t \ge t_i \ . \tag{2.1.10}$$

Hypothesis 1.3.1 is concerned with how these increments can be combined to give the actual stress $\sigma(x,t)$ at position x and time t and it states that these increments can be added in a linear way to give

$$\begin{aligned}\sigma(x,t) = \sum_{i=0}^{N-1} \Delta\sigma^i(x,t) &= \sum_{i=0}^{N-1} D(x,t-t_i)\Delta\varepsilon(x,t_i) \\ &= \sum_{i=0}^{N-2} \Big(D(x,t-t_i) - D(x,t-t_{i+1})\Big)\varepsilon(x,t_i) + D(x,t-t_{N-1})\varepsilon(x,t_{N-1}) \ .\end{aligned} \tag{2.1.11}$$

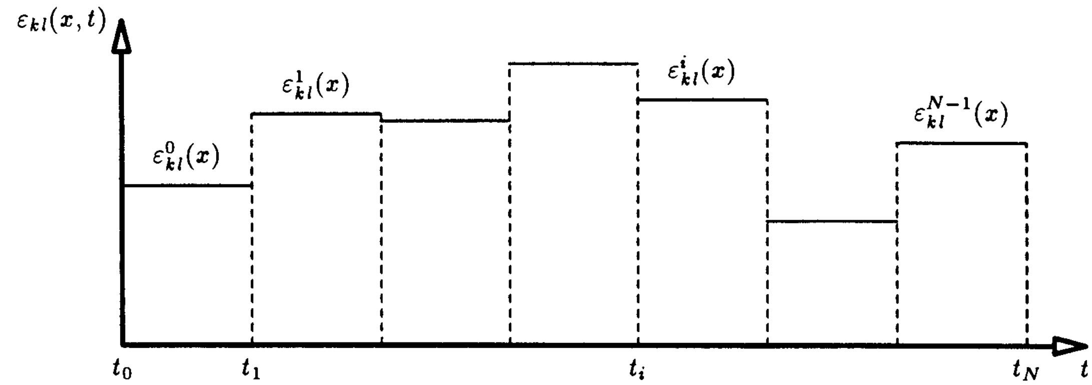

Figure 2.1.1 The step function for the kl component of strain

If D is continuously differentiable with respect to its time argument then extending this idea to the limit as $N \to \infty$ with $t_N \to t$ and $\max_i(t_i - t_{i-1}) \to 0$ in the usual way gives, using the last part of (2.1.11),

$$\sigma(x,t) = D(x,0)\varepsilon(x,t) - \int_{t_0}^{t} \frac{\partial D(x,t-\tau)}{\partial\tau}\varepsilon(x,\tau)\, d\tau \ . \tag{2.1.12}$$

In the case of a smooth deformation, specifically for which $\partial\varepsilon/\partial\tau$ exists except possibly for an initial jump discontinuity of ε at t_0, the limiting argument just described gives, using the previous part of (2.1.11),

$$\sigma(x,t) = D(x,t-t_0)\varepsilon(x,t_0) + \int_{t_0}^{t} D(x,t-\tau)\frac{\partial\varepsilon}{\partial\tau}(x,\tau)\, d\tau \ . \tag{2.1.13}$$

Note that (2.1.13) could have been formally derived from (2.1.12) by integration by parts (and *vice-versa*) and also both forms are implicitly applicable only to non-ageing materials since the stress relaxation matrix D depends only upon the relative or elapsed time.

Next we generalise to the case of an ageing material by generalising the arguments of D. Specifically we take D to have the 3 arguments x, t and τ where x is position, t is the current time and $\tau \leq t$ is a previous time and we define the constitutive relations

$$\begin{aligned}\sigma(x,t) &= D(x,t,0)\varepsilon(x,0) + \int_0^t D(x,t,\tau)\varepsilon'(x,\tau)\, d\tau \\ &= D(x,t,t)\varepsilon(x,t) - \int_0^t D'(x,t,\tau)\varepsilon(x,\tau)\, d\tau,\end{aligned} \tag{2.1.14}$$

where we have assumed for convenience that $t_0 = 0$ and $'$ denotes differentiation with respect to τ. In component form the relation can be written as

$$\sigma_{ij}(x,t) = \lambda(x,t,t)\nabla\cdot u(x,t)\delta_{ij} + \mu(x,t,t)\varepsilon_{ij}\big(u(x,t)\big) - \int_0^t \lambda'(x,t,\tau)\nabla\cdot u(x,\tau)\delta_{ij} + \mu'(x,t,\tau)\varepsilon_{ij}\big(u(x,\tau)\big)\, d\tau, \tag{2.1.15}$$

or

$$\sigma_{ij}(x,t) = \lambda(x,t,0)\nabla\cdot u(x,0)\delta_{ij} + \mu(x,t,0)\varepsilon_{ij}\big(u(x,0)\big) + \int_0^t \lambda(x,t,\tau)\nabla\cdot u'(x,\tau)\delta_{ij} + \mu(x,t,\tau)\varepsilon_{ij}\big(u'(x,\tau)\big)\, d\tau, \tag{2.1.16}$$

Unless specifically stated otherwise the Einstein summation convention, as used here, will be used in all that follows.

The functions $\lambda(x,t,\tau)$ and $\mu(x,t,\tau)$ are the viscoelastic analogues of the Lamé coefficients that appear in linear elasticity (2.1.4). The time dependent parts of these functions arise from the stress relaxation functions characterizing the material. We must assume that these functions exist and that they, in general, will vary for different modes of deformation, for example bulk or shear. However, for a non-ageing material any pair of these is, in principle, sufficient to determine the time dependent parts of λ and μ via the correspondence principle [3,4]. The spatial, x, dependence of λ and μ will usually be of little interest but is retained here for generality.

To facilitate the forthcoming error analysis we make the following, physically reasonable, assumptions on λ and μ:

Assumptions 2.1.1.

i) For every fixed $t \in \mathcal{I}$ and τ such that $t-\tau \in \mathcal{I}$

$$\lambda(x,t,\tau),\ \mu(x,t,\tau) \in \mathcal{H}^m\Big(\{t-\tau\in\mathcal{I}\};\mathcal{L}_2(\Omega)\bigcap\mathcal{L}_\infty(\Omega)\Big)\bigcap\mathcal{W}^{1,\infty}\Big(\{t-\tau\in\mathcal{I}\};\mathcal{L}_\infty(\Omega)\Big),$$

where we assume m may be taken sufficiently large for the following analysis to remain valid. So on a physical basis we expect λ and μ to be well behaved in time, but must allow for material property variation in space. This would be the case if, for example, two different materials were mechanically joined in some structure.

ii) For every $t \in \mathcal{I}$: $0 < \lambda(x,t,\tau),\ \mu(x,t,\tau)\quad \forall x \in \overline{\Omega}$ and $\forall t-\tau \in \mathcal{I}$.

iii) For every $t \in \mathcal{I}$: $0 < \lambda'(x,t,\tau),\ \mu'(x,t,\tau)\quad \forall x \in \overline{\Omega}$ and $\forall t-\tau \in \mathcal{I}$.

iv) Causality: $\forall t \in \mathcal{I}\quad \lambda(x,t,\tau),\mu(x,t,\tau) \equiv 0$ if $\tau > t$. This simply means that we do not allow future events in the deformation history to affect present behaviour. ∎

2.2 Two weak formulations: $\mathbf{P}_1$ and $\mathbf{P}_2$.

Based on the law of conservation of momentum we consider the quasistatic equations of equilibrium

$$-\sum_{j=1}^{n}\frac{\partial\sigma_{ij}}{\partial x_j}(x,t) = f_i(x,t),\ i=1,\ldots,n,\ x\in\Omega,\ t\in\mathcal{I}, \tag{2.2.1}$$

with the boundary conditions

$$u(x,t) = 0,\quad x\in\Gamma^D \neq \emptyset,\ t\in\mathcal{I}, \tag{2.2.2}$$

$$\sum_{j=1}^{n}\sigma_{ij}\hat{n}_j(x,t) = g_i(x,t),\quad x\in\Gamma^N,\ t\in\mathcal{I},\ i=1,\ldots,n. \tag{2.2.3}$$

Where $\Gamma^D\bigcup\Gamma^N \equiv \partial\Omega$ and $\hat{n} := (\hat{n}_j)_{j=1}^n$ is the unit outward normal to $\partial\Omega$. A weak formulation of (2.2.1, ..., 3) is formed by taking the scalar product of (2.2.1) with a test function $v := (v_i)_{i=1}^n \in \mathcal{V}$, where $\forall t \in \mathcal{I}$

$$\mathcal{V} := \Big\{v \in \big(\mathcal{H}^1(\Omega)\big)^n : v(x) = 0\ \forall x\in\Gamma^D\Big\}. \tag{2.2.4}$$

Integrating by parts [5] we produce the weak formulation in which we seek $u \in \mathcal{V}$ at each $t\in\mathcal{I}$ such that

$$\int_\Omega \sigma(u;x,t)\cdot\varepsilon\big(v(x)\big)\, dx = \int_\Omega f\cdot v\, dx + \int_{\partial\Omega} g\cdot v\, ds,\ \forall v\in\mathcal{V}, \tag{2.2.5}$$

where $\cdot$ indicates the Euclidean inner product and the "test strain" is given by

$$\varepsilon_{ij}(v) := \frac{1}{2}\left(\frac{\partial v_i}{\partial x_j} + \frac{\partial v_j}{\partial x_i}\right) \ \forall v \in \mathcal{V}, \qquad 0 \le i, j \le n. \tag{2.2.6}$$

Use of the constitutive relationships (2.1.15) and (2.1.16) enables two alternative weak formulations, $\mathbf{P}_1$ and $\mathbf{P}_2$, of the quasistatic linear viscoelastic stress analysis problem to be defined. For notational convenience, we let

$$a(\lambda(x,t,\tau), \mu(x,t,\tau), u(x,t,\tau)) = \int_\Omega \lambda(x,t,\tau)\nabla\cdot u(x,t)\nabla\cdot v(x) + \mu(x,t,\tau)\varepsilon_{ij}(u(x,\tau))\varepsilon_{ij}(v(x)) \ dx \tag{2.2.7}$$

which is essentially just the usual bilinear form used to describe linear elasticity. The two problems are then as follows.

$\mathbf{P}_1$: Find $u(x,t) \in \mathcal{L}_2(\mathcal{I}; \mathcal{V})$ such that

$$a\big((\lambda(x,t,t), \mu(x,t,t), u(x,t)), v(x)\big) - \int_0^t a\big((\lambda'(x,t,\tau), \mu'(x,t,\tau), u(x,\tau)), v(x)\big) \ d\tau = l(v;t) \quad \forall v \in \mathcal{V} \text{ and } \forall t \in \mathcal{I}. \tag{2.2.8}$$

$\mathbf{P}_2$: Find $u(x,t) \in \mathcal{H}^1(\mathcal{I}; \mathcal{V})$ such that

$$a\big((\lambda(x,t,0), \mu(x,t,0), u(x,0), v(x)\big) + \int_0^t a\big((\lambda(x,t,\tau), \mu(x,t,\tau), u'(x,\tau)), v(x)\big) \ d\tau = l(v;t) \quad \forall v \in \mathcal{V} \text{ and } \forall t \in \mathcal{I}, \tag{2.2.9}$$

where $l(v;t) := (f(x,t), v)_\Omega + (g(x,t), v)_{\partial\Omega}$, and $(\cdot,\cdot)_\mathcal{B}$ is the inner product on $\mathcal{L}_2(\mathcal{B})$. In each case we have assumed that it is permissable to interchange the order of spatial and temporal integration. In much of the following the x dependence of λ and μ will not be indicated explicitly.

In order to facilitate the analysis we first state some assumptions, give some notation and state three inequalities which will be required.

Assumptions 2.2.1.

i). For $\mathbf{P}_1$ and $\mathbf{P}_2$: $f(x,t) \in \mathcal{L}_2\big(\mathcal{I}; (\mathcal{L}_2(\Omega))^n\big)$.

ii). For $\mathbf{P}_1$ and $\mathbf{P}_2$: $g(x,t) \in \mathcal{L}_2\big(\mathcal{I}; (\mathcal{H}^{\frac{1}{2}}(\partial\Omega))^{n-1}\big)$. ∎

Definition 2.2.1. For $v_i \in \mathcal{H}^p(\Omega)$ we have

$$\|v_i\|_{p,\Omega} := \left(\sum_{|\alpha|\le p} \|D^\alpha v_i\|^2_{\mathcal{L}_2(\Omega)}\right)^{1/2}. \qquad ∎$$

Definition 2.2.2. For $v \in \big(\mathcal{H}^p(\Omega)\big)^m$ we have

$$\|v\|_{p,\Omega} := \left(\sum_{i=1}^m \|v_i\|^2_{p,\Omega}\right)^{1/2}. \qquad ∎$$

Definition 2.2.3. For $v \in \mathcal{L}_2\big(\mathcal{I}; \mathcal{H}^p(\Omega)\big)$ we have

$$\|v\|_{\mathcal{L}_2(\mathcal{I};\mathcal{H}^p)} := \left(\int_\mathcal{I} \|v\|^2_{p,\Omega}(\tau) \ d\tau\right)^{1/2}. \qquad ∎$$

Lemma 2.2.1. *Korn's inequality [8], for $v \in \left(\mathcal{H}^1(\Omega)\right)^m$, and ε_{ij} defined by (2.2.6) we have*

$$\sum_{i,j=1}^{m} \int_\Omega \varepsilon_{ij}(v)\varepsilon_{ij}(v)\ dx \geq C\|v\|_{1,\Omega}^2,$$

for some constant $C > 0$. ∎

Lemma 2.2.2. *Continuous Gronwall inequality [9,12]. Let u, v, w be piecewise continuous non-negative functions defined on the interval $t \in [0,a]$, v being non-decreasing. If, for each $t \in [0,a]$, $\exists C > 0$, independent of t, such that*

$$u(t) + w(t) \leq v(t) + C \int_0^t u(s)\ ds,$$

then

$$u(t) + w(t) \leq v(t) \exp(Ct)\ .$$ ∎

Lemma 2.2.3. *Discrete Gronwall inequality [9]. Let u, v, w be non-negative functions defined on*

$$\mathcal{J}_k := \left\{t \in \mathcal{R} : t = jk;\ j = 0, 1, \ldots, J;\ T = Jk\right\}$$

with $v(t)$ being non-decreasing and $k > 0$ being constant. If, for each $t \in \mathcal{J}_k$, $\exists C > 0$, independent of t, such that

$$u(t) + w(t) \leq v(t) + Ck \sum_{\tau=0}^{t-k} u(\tau),$$

then

$$u(t) + w(t) \leq v(t) \exp(Ct)\ .$$ ∎

Remark 2.2.1. Under very mild restrictions on λ and μ which are covered by assumption 2.1.1, it can be shown that $a\big((\lambda, \mu, \ \cdot\ ), \ \cdot\ \big)$ is a symmetric continuous $\mathcal{V}$-elliptic bilinear form for each $t, t-\tau \in \mathcal{I}$ see, for example [6]. The $\mathcal{V}$-ellipticity may be shown by first observing that

$$\exists C(t) \in [0,3] \text{ such that } \|\nabla \cdot u\|_{0,\Omega}^2 \leq C(t)\|u\|_{1,\Omega}^2 \quad \forall u \in \mathcal{V},$$

and then using the Korn inequality (lemma 2.2.1) to write:

$$\int_\Omega \lambda \nabla \cdot u \nabla \cdot u\ dx + \int_\Omega \mu \varepsilon_{ij}(u)\varepsilon_{ij}(u)\ dx \geq \left(\tilde{\lambda}(t) + \tilde{\mu}(t)\right)\|u\|_{1,\Omega}^2,$$

where $\tilde{\mu}(t) > 0$ by assumption 2.1.1. ∎

Assumption 2.2.2. We shall assume throughout that there exists a unique $u(x,t) \in \mathcal{L}_2(\mathcal{I}; \mathcal{V})$ that solves $\mathbf{P}_1$. This in fact may be shown using the *Picard* iteration, detailed by Linz [13], and exploiting the $\mathcal{V}$-ellipticity of $a\big((\lambda, \mu, \cdot\ ), \cdot\ \big)$. ∎

3 Semi-discrete formulation.

3.1 Preliminary notation.

In this section we define semi-discrete problems approximating $\mathbf{P}_1$ and $\mathbf{P}_2$ by forming their corresponding finite element approximations in space. For this the region Ω is partitioned into M_e disjoint finite elements Ω_i^h such that $\forall t \in \mathcal{I}$

$$\partial\Omega^h \equiv \partial\Omega \text{ and } \Omega^h := \bigcup_{i=1}^{M_e} \Omega_i^h, \tag{3.1.1}$$

i.e. the partition does not change with time. Also we define over this partition the finite dimensional space

$$\mathcal{V}^h := \left\{v^h \in \mathcal{V} : \; v^h|_{\Omega_i^h} \in \left(\mathcal{P}_p(x)\right)^n, \; 1 \le i \le M_e\right\}, \tag{3.1.2}$$

where, $\left(\mathcal{P}_p(x)\right)^n$ denotes the set of p^{th} order complete polynomials in the variables $(x_j)_{j=1}^n$.

We will approximate the weak solution $u(x,t)$ to either of (2.2.8) or (2.2.9) by $u^h(x,t)$ written in terms of the basis functions $\{\phi_j(x)\}_{j=1}^{M^h}$ defined over Ω^h. Specifically we have

$$\left(u^h(x,t)\right)_i = \sum_{j=1}^{M^h} \phi_j(x) L_{ji}(u^h(x,t)),$$

where $M^h > 0$ is an integer depending upon the partition relating to the number of nodal parameters (usually this will simply be just the number of nodes.) and L_{ji} is the operator which extracts the i^{th} displacement component associated with the j^{th} basis function for the finite element approximation. In this way, for a given $t \in \mathcal{I}$ we write

$$u^h(x,t) = N(x)U(t), \tag{3.1.4}$$

where for any $x \in \Omega$ and any $t \in \mathcal{I}$

$$\begin{aligned}
\left(U(t)\right)^T &= \left(L_{11}(u^h(x,t)) \ldots L_{M^h n}(u^h(x,t))\right) \in \mathcal{R}^{nM^h} \\
N(x) &= [\Phi_1(x) \;\; \cdots \;\; \Phi_{M^h}(x)] \in \left(\mathcal{H}^1(\cup_i \Omega_i^h)\right)^{n,nM^h}, && (3.1.6) \\
\Phi_i(x) &= I\phi_i(x) && (3.1.7)
\end{aligned}$$

where I is the identity on $\mathcal{R}^n$. Using (2.1.3) we define the approximate strain as

$$\varepsilon^h\left(u^h(x,t)\right) = B(x)U(t) \tag{3.1.8}$$

where $B(x) \in \left(\mathcal{L}_2(\Omega)\right)^{n(n+1)/2,nM^h}$ is a matrix whose entries consist of derivatives of the basis functions.

3.2 Semi-discretization of $\mathbf{P}_1$, and error analysis.

3.2.1 Semi-discretization.

The approximate stress is defined via (2.1.15) and (3.1.8) yielding

$$\sigma^h(u^h; x,t) = D(x,t,t)B(x)U(t) - \int_0^t D'(x,t,\tau)B(x)U(\tau)\, d\tau. \tag{3.2.1}$$

We then have the semi-discrete approximation to $\mathbf{P}_1$:

$\mathbf{P}_1^h$: Find $u^h(x,t) \in \mathcal{L}_2(\mathcal{I}; \mathcal{V}^h)$ such that

$$\begin{aligned}
&a\big((\lambda(x,t,t), \mu(x,t,t), u^h(x,t)), v^h(x)\big) \\
&\quad - \int_0^t a\big((\lambda'(x,t,\tau), \mu'(x,t,\tau), u^h(x,\tau)), v^h(x)\big)\, d\tau = l(v^h;t) \qquad \forall v^h \in \mathcal{V}^h,
\end{aligned} \tag{3.2.2}$$

which may be written as

$$A(t,t)U(t) - \int_0^t A'(t,\tau)U(\tau)\, d\tau = F(t), \tag{3.2.3}$$

where A is the positive definite (due to (2.2.2) and assumption 2.1.1) finite element stiffness matrix defined by

$$A(t,s) := \int_{\Omega^h} B^T(x)D(x,t,s)B(x)\, dx. \tag{3.2.4}$$

Remark 3.2.1. Note that (3.2.3) may be written as

$$U(t) = G(t) + \int_0^t K(t,\tau)U(\tau)\,d\tau,$$

where

$$G(t) := \big(A(t,t)\big)^{-1}F(t) \in \big(\mathcal{L}_2(\mathcal{I})\big)^N,$$
$$K(t,\tau) = \big(A(t,t)\big)^{-1}A'(t,\tau) \in \big(\mathcal{L}_2(\mathcal{I})\big)^{N,N},$$

for an integer N depending upon the partition of Ω and the value of n. The assumptions 2.1.1 and 2.2.1 ensure that there exists $U(t) \in \mathcal{L}_2(\mathcal{I})$ that solves (3.2.3), see for example Tricomi [10] where the analysis for a scalar equation is given. ∎

3.2.2 Error analysis.

In this section we derive a $\mathcal{H}^1$-error estimate for the semi-discrete approximation $u^h(x,t)$, given by (3.2.2), to the solution $u(x,t)$ of (2.2.8), for this we employ the technique of elliptic projection, see [7]. For any $t \in \mathcal{I}$ the elliptic projection $\tilde{u}^h(x,t) \in \mathcal{L}_2(\mathcal{I}, \mathcal{V}^h)$ of $u(x,t)$, the solution to (2.2.8), onto the test space $\mathcal{V}^h$ is defined by

$$a\big((\lambda(x,t,t), \mu(x,t,t), u(x,t) - \tilde{u}^h(x,t)), v^h\big) = 0 \qquad \forall v^h \in \mathcal{V}^h. \tag{3.2.5}$$

If we define

$$\eta := u - \tilde{u}^h, \qquad \zeta := \tilde{u}^h - u^h,$$

set $v = v^h$ in (2.2.8), subtract (3.2.2), use the projection (3.2.5) and omit the implicit dependence on x for clarity we have:

$$a\big((\lambda(t,t), \mu(t,t), \zeta(t)), v^h\big) = \int_0^t a\big((\lambda'(t,\tau), \mu'(t,\tau), \eta(\tau)), v^h\big)\,d\tau$$
$$+ \int_0^t a\big((\lambda'(t,\tau), \mu'(t,\tau), \zeta(\tau)), v^h\big)\,d\tau. \tag{3.2.6}$$

Since we seek to estimate the error $\|u - u^h\|_{1,\Omega}$, using the above definitions we have immediately that, for $t \in \mathcal{I}$,

$$\|u(x,t) - u^h(x,t)\|_{1,\Omega} \le \|\eta(x,t)\|_{1,\Omega} + \|\zeta(x,t)\|_{1,\Omega}, \tag{3.2.7}$$

and the task is now that of bounding the terms η and ζ in the norm $\|\cdot\|_{1,\Omega}$.

Now, for any $t \in \mathcal{I}$, we choose $v^h = \zeta(t)$ in (3.2.6) and observe that remark 2.2.1 gives a $C_1(t) > 0$, thus allowing (3.2.6) to be written as

$$C_1\|\zeta(t)\|_{1,\Omega}^2 \le \int_0^t a\big((\lambda'(t,\tau), \mu'(t,\tau), \eta(\tau)), \zeta(t)\big)\,d\tau$$
$$+ \int_0^t a\big((\lambda'(t,\tau), \mu'(t,\tau), \zeta(\tau)), \zeta(t)\big)\,d\tau. \tag{3.2.8}$$

We proceed by noting the following

Lemma 3.2.1. Define the symbol $b(\cdot\,,\cdot\,,\cdot\,)$ by

$$b(\phi, \nabla\cdot\eta, \nabla\cdot\zeta) := \int_0^t \int_\Omega \phi(x,t,s)\nabla\cdot\eta(x,s)\nabla\cdot\zeta(x,t)\,dx ds$$

where

$$\phi(x,t,s) \in \mathcal{L}_2\big((0,t);\mathcal{L}_\infty\big) \text{ for each } t \in \mathcal{I}$$
$$\eta(x,s) \in \mathcal{L}_2\big((0,t);(\mathcal{H}^1(\Omega))^n\big)$$
$$\zeta(x,t) \in \big(\mathcal{H}^1(\Omega)\big)^n \text{ for each } t \in \mathcal{I}.$$

Then

$$b(\phi, \nabla\cdot\eta, \nabla\cdot\zeta) \leq \|\hat{\phi}(s)\|_{0,(0,t)}\|\zeta(t)\|_{1,\Omega}\|\eta(s)\|_{\mathcal{L}_2((0,t);(\mathcal{H}^1(\Omega))^n)} \quad \forall t \in \mathcal{I},$$

where

$$\hat{\phi}(s) = \operatorname*{ess\ sup}_{x\in\Omega} \phi(x, s).$$

Proof. Interchanging the order of integration and liberally applying the Cauchy-Schwartz inequality gives

$$\begin{aligned} b(\phi, \nabla\cdot\eta, \nabla\cdot\zeta) &= \int_\Omega \left(\int_0^t \phi(s)\nabla\cdot\eta(s)\ ds \right) \nabla\cdot\zeta(t)\ dx \\ &\leq \|\zeta\|_{1,\Omega}\left[\int_\Omega \left(\int_0^t \phi(s)\nabla\cdot\eta(s)\ ds \right)^2 dx \right]^{1/2} \\ &\leq \|\zeta\|_{1,\Omega}\left[\int_\Omega \|\phi\|^2_{0,(0,t)}\ \|\nabla\cdot\eta\|^2_{0,(0,t)}\ dx \right]^{1/2} \\ &\leq \|\hat{\phi}\|_{0,(0,t)}\|\zeta\|_{1,\Omega}\|\eta\|_{\mathcal{L}_2((0,t);(\mathcal{H}^1(\Omega))^n)}. \end{aligned}$$

■

Noting the definition of $a\big((\lambda, \mu, \cdot\,), \cdot\,\big)$ and applying lemma 3.2.1, coupled with an almost identical argument for the ε terms (i.e. consider $b\big(\phi, \varepsilon(\eta), \varepsilon(\zeta)\big)$ in the lemma), we write (3.2.8) as

$$\|\zeta(t)\|_{1,\Omega} \leq C_2\Big(\|\eta(\tau)\|_{\mathcal{L}_2((0,t);\mathcal{H}^1(\Omega))^n)} + \|\zeta(\tau)\|_{\mathcal{L}_2((0,t);(\mathcal{H}^1(\Omega))^n)}\Big) \tag{3.2.9}$$

with

$$C_2 = \check{C}_1^{-1}\Big(\|\hat{\lambda}'\|_{0,(0,t)} + 9\|\hat{\mu}'\|_{0,(0,t)}\Big) \tag{3.2.10}$$

$$\check{C}_1 := \inf_{t-\tau\in[0,t]} C_1. \tag{3.2.11}$$

Squaring both sides of (3.2.9) and using the inequality

$$2ab \leq a^2 + b^2 \qquad \forall a, b \in \mathcal{R}, \tag{3.2.12}$$

we have by Gronwall's inequality (lemma 2.2.2)

$$\begin{aligned} &\|\zeta(t)\|^2_{1,\Omega} \leq 2C_2^2\|\eta(\tau)\|^2_{\mathcal{L}_2((0,t);(\mathcal{H}^1(\Omega))^n)} + 2C_2^2\|\zeta(\tau)\|^2_{\mathcal{L}_2((0,t);(\mathcal{H}^1(\Omega))^n)} \\ \Rightarrow\quad &\|\zeta(t)\|_{1,\Omega} \leq C_3\|\eta(\tau)\|_{\mathcal{L}_2((0,t);(\mathcal{H}^1(\Omega))^n)}\exp(C_2^2 t), \quad \text{where} \quad C_3 := \sqrt{2}C_2. \end{aligned} \tag{3.2.13}$$

Assuming a suitable discretisation of the domain Ω and using assumptions 2.2.1 we have, see [6], constants $C_\eta > 0$ and $\alpha > 0$, depending upon the regularity of the weak solution, the degree p of the approximating polynomials and the mesh partition (i.e. the space $\mathcal{V}^h$.), such that

$$\begin{aligned} \|\eta(x,t)\|_{1,\Omega} &\leq C \inf_{v^h\in\mathcal{V}^h} \|u - v^h\|_{1,\Omega} \\ &\leq C_\eta h^\alpha |u(x,t)|_{1+\alpha,\Omega} \quad \forall t \in \mathcal{I}, \end{aligned} \tag{3.2.14}$$

where

$$h := \max_{1\leq i\leq M_e} \ \text{diam}\ \Omega_i^h.$$

Hence, we have the following semi-discrete error estimate:

Theorem 3.2.1. *Assuming that* $u \in \mathcal{L}_2(\mathcal{I};\mathcal{V})\bigcap\mathcal{L}_2\big(\mathcal{I};\big(\mathcal{H}^{1+\alpha}(\Omega)\big)^n\big)\bigcap\mathcal{L}_\infty\big(\mathcal{I};\big(\mathcal{H}^{1+\alpha}(\Omega)\big)^n\big)$ *and that* $\tilde{u}^h \in \mathcal{L}_\infty(\mathcal{I};\mathcal{V}^h)\bigcap\mathcal{L}_2(\mathcal{I};\mathcal{V}^h)$, *and observing assumptions 2.1.1, then for the error associated with* $\mathbf{P}_1^h$, *the semi-discrete aproximation to* $\mathbf{P}_1$, $\forall t \in \mathcal{I}\ \ \exists C \geq 0$ *depending upon* u *but independent of* h *such that*

$$\|u(x,t) - u^h(x,t)\|_{1,\Omega} \leq Ch^\alpha.$$

Proof. *Use (3.2.7) with (3.2.13,14) to write at any $t \in \mathcal{I}$:*

$$\begin{aligned}\|u(x,t)-u^h(x,t)\|_{1,\Omega} &\le C_\eta h^\alpha |u(x,t)|_{1+\alpha,\Omega} + C_3 C_\eta h^\alpha |u(x,\tau)|_{\mathcal{L}_2((0,t);(\mathcal{H}^{1+\alpha}(\Omega))^n)} \exp(C_2^2 t/2)\\ &\le C_\eta h^\alpha |u(x,\tau)|_{\mathcal{L}_\infty(\mathcal{I};(\mathcal{H}^{1+\alpha}(\Omega))^n)} + \hat{C}_3 C_\eta h^\alpha |u(x,\tau)|_{\mathcal{L}_2(\mathcal{I};(\mathcal{H}^{1+\alpha}(\Omega))^n)} \exp(\hat{C}_2^2 t/2)\\ &\le C h^\alpha\end{aligned}$$

where

$$\hat{C}_2 := \sup_{t-\tau\in\mathcal{I}} C_2.$$

and

$$\hat{C}_3 := \sup_{t-\tau\in\mathcal{I}} C_3,$$

The existence of $\hat{C}_2$ and $\hat{C}_3$ are guaranteed by assumption 2.1.1 and remark 2.2.1. ∎

3.3 Semi-discretization of $\mathbf{P}_2$, and error analysis.

3.3.1 Semi-discretization.

Again using (3.1.8) but this time with (2.1.16) we define the approximate stress through

$$\sigma^h(u^h;x,t) = D(x,t,0)B(x)U(0) + \int_0^t D(x,t,\tau)B(x)U'(\tau)\,d\tau. \tag{3.3.1}$$

In which case we have

$\mathbf{P}_2^h$: Find $u^h(x,t) \in \mathcal{V}^h$ for each $t \in \mathcal{I}$ such that

$$\begin{aligned}&a\big((\lambda(x,t,0),\mu(x,t,0),u^h(x,0)),v^h(x)\big)\\ &\quad+\int_0^t a\big((\lambda(x,t,\tau),\mu(x,t,\tau),(u^h(x,\tau))'),v^h(x)\big)\,d\tau = l(v^h;t) \qquad \forall v^h \in \mathcal{V}^h,\end{aligned} \tag{3.3.2}$$

which may be written as

$$\int_0^t A(t,\tau)U'(\tau)\,d\tau = b(t), \tag{3.3.3}$$

where

$$b(t) := F(t) - A(t,0)U(0). \tag{3.3.4}$$

The initial condition $U(0)$ is found via the equation $b(0) = 0$, i.e. by solving a problem of linear elasticity at $t = 0$. In this case we have produced a Volterra integral equation of the first kind for $U'(t)$.

3.3.2 Error analysis.

As a rule Volterra integral equations of the first kind are rather more difficult to deal with than those of the second kind (see for example [10,13]), moreover once the initial condition has been determined (2.2.9) is actually an integrodifferential equation for $u(x,t)$ of a non-standard type. We have not attempted a direct semi-discrete error analysis for $\mathbf{P}_2$ here, but choose instead to rely on the observation that if the numerical algorithm promised by $\mathbf{P}_2$ is to be useful then $u'(x,t)$ is required to exist, at least in the weak sense, and so we may simply state:

Theorem 3.3.1. *If the conditions required for theorem 3.2.1 are satisfied with the further condition that $u(x,t) \in \mathcal{W}^{1,1}(\mathcal{I};\mathcal{V}) \bigcap \mathcal{L}_2(\mathcal{I};\mathcal{V}) \bigcap \mathcal{L}_2(\mathcal{I};(\mathcal{H}^{1+\alpha}(\Omega))^n) \bigcap \mathcal{L}_\infty(\mathcal{I};(\mathcal{H}^{1+\alpha}(\Omega))^n)$ – a sufficient condition for this extra regularity in time may be provided by strengthening assumption 2.2.1 to $f(x,t) \in C^1(\mathcal{I};(\mathcal{L}_2(\Omega))^n)$ and $g(x,t) \in C^1(\mathcal{I};(\mathcal{H}^{\frac{1}{2}}(\partial\Omega))^{n-1})$, then for the error associated with $\mathbf{P}_2^h$, the semidiscrete approximation to $\mathbf{P}_2$, $\exists C \ge 0 \quad \forall t \in \mathcal{I}$ such that*

$$\|u(x,t) - u^h(x,t)\|_{1,\Omega} \le C h^\alpha,$$

and this C is the same as that appearing in theorem 3.2.1.

Proof. *Integrate (2.2.9) by parts to yield (2.2.8) and (3.3.2) to yield (3.2.2), because of the uniqueness, assumption 2.2.2, the result of theorem 3.2.1 may be applied.* ∎

4 Fully discrete formulation.

4.1 Preamble.

To provide fully discrete approximations to $\mathbf{P}_1^h$ and $\mathbf{P}_2^h$ we use respectively the trapezoidal rule for numerical integration and a type of product integration rule coupled with a finite difference replacement. In the ensuing analysis we assume, in both cases, a constant time step $k := t_i - t_{i-1}, i = 1, \ldots, I$. The time domain $\mathcal{I}$ is discretized into

$$\mathcal{I}^k := \left\{0 = t_0, \ \cdots, t_i, \ \cdots, t_I \in \mathcal{R} : \text{ and } t_i > t_{i-1} \text{ for } 1 \leq i \leq I\right\} \subset \mathcal{I}. \tag{4.1.1}$$

4.2 Full discretization.

4.2.1 Full discretization of $\mathbf{P}_1$.

In order to present a fully discrete scheme for $\mathbf{P}_1$ we need to discretize $\mathbf{P}_1^h$ in time, for this we utilise the trapezoidal rule for numerical integration, the generic form of which is:

$$\delta(k, t_j) = \int_0^{t_j} y(x)\ dx - \sum_{i=1}^{j} \frac{k_i}{2}\left(y_{i-1} + y_i\right), \tag{4.2.1}$$

where

$$\begin{aligned} y_i &:= y(x_i), \\ k_i &:= x_i - x_{i-1}, \quad 1 \leq i \leq j \leq I, \end{aligned} \tag{4.2.2}$$

Then by setting

$$k = \max_{1 \leq i \leq j} \left\{k_i\right\}, \tag{4.2.3}$$

and assuming appropriate continuity of y, δ may be estimated by

$$|\delta(k, t_j)| \leq C_j k^2 |y''(\xi)|, \qquad \text{for some } \xi \in (0, t_j). \tag{4.2.4}$$

Thus, we replace the integral occuring in (3.2.3) with the trapezoidal approximation, neglect the error term δ, and arrive at:

$\mathbf{P}_1^{h,k}$: Find $\left(u^h(x)\right)_j \in \mathcal{V}^h$ for each $t_j \in \mathcal{I}^k$ such that

$$A(t_j, t_j)U_j - \sum_{q=1}^{j} \frac{k_q}{2}\left(A'(t_j, t_q)U_q + A'(t_j, t_{q-1})U_{q-1}\right) = F_j. \tag{4.2.5}$$

Rearranging this equation to

$$\left(A(t_j, t_j) - \frac{k_j}{2}A'(t_j, t_j)\right)U_j = F_j + \frac{k_j}{2}A'(t_j, t_{j-1})U_{j-1} + \sum_{q=1}^{j-1} \frac{k_q}{2}\left(A'(t_j, t_q)U_q + A'(t_j, t_{q-1})U_{q-1}\right)$$

and taking k_j small enough for the left hand side term to be invertible allows successive solution for $U_0, U_1, \ \ldots, U_I$, thus yielding the approximation to $u^h(x, t)$ by substituting U_j for $U(t_j)$ in (3.1.4) giving $\left(u^h(x)\right)_j$. We note here that the trapezoidal method does not require starting values and is not restricted to constant k as higher order methods would be. Also, since the scheme has a repetition factor of 1 it is numerically stable in sense of Linz, see for example [13,14].

4.2.2 Completion of the error estimate for $\mathbf{P}_1$.

To build upon the semi-discrete error estimate of theorem 3.2.1 we will denote the fully discrete solution to $\mathbf{P}_1^{h,k}$ at each $t_i \in \mathcal{I}^k$ by $\left(u^h(x)\right)_i$ and also define $\theta(x, t_r) := u^h(x, t_r) - \left(u^h(x)\right)_r \ \forall t_r \in \mathcal{I}^k$. We then have

$$\|u(x, t_r) - \left(u^h(x)\right)_r\| \leq \|u(x, t_r) - u^h(x, t_r)\| + \|\theta(x, t_r)\|. \tag{4.2.6}$$

As the first term on the right hand side of (4.2.6) has been bounded in theorem 3.2.1 we now seek an estimate for θ in the $\|\cdot\|_{1,\Omega}$ norm. Assuming a constant time step k, (4.2.5) may be written

as:
Find $\left(u^h(x)\right)_r \in \mathcal{V}^h$ for each $t_r \in \mathcal{I}^k$ such that $\forall v^h \in \mathcal{V}^h$

$$a\big((\lambda(t_r,t_r),\mu(t_r,t_r),(u^h)_r),v^h\big) - k\sum_{q=0}^{r} w_{rq}a\big((\lambda'(t_r,t_q),\mu'(t_r,t_q),(u^h)_q),v^h\big) = F_r, \qquad (4.2.7)$$

where the w_{rq} are the weights associated with the trapezoidal rule (4.2.1). Subtraction of (4.2.7) from (3.2.2) evaluated at $t = t_r$ gives (using (4.2.1))

$$a\big((\lambda(t_r,t_r),\mu(t_r,t_r),\theta(t_r)),v^h\big) = \delta(k,t_r) + k\sum_{q=0}^{r} w_{rq}\ a\big((\lambda'(t_r,t_q),\mu'(t_r,t_q),\theta(t_q)),v^h\big) \quad (4.2.8)$$

and, assuming certain smoothness in time, specifically $u^h(x,\cdot) \in \mathcal{C}^2(\mathcal{I})$(for this it is sufficient to strengthen assumption 2.2.1 such that $l(v;\cdot) \in \mathcal{C}^2(\mathcal{I})$, see for example [13].)

$$\delta(k,t_r) = C_r k^2 \frac{\partial^2}{\partial\tau^2} a\big((\lambda'(t_r,\tilde\tau),\mu'(t_r,\tilde\tau),u^h(x,\tilde\tau)),v^h\big),\ \tilde\tau \in [0,t_r]. \qquad (4.2.9)$$

We choose $v^h = \theta_r := \theta(t_r) \in \mathcal{V}^h$ and again use the $\mathcal{V}$-ellipticity (remark 2.2.1) on the term on the left hand side of (4.2.8) giving a constant $C_1(t) > 0$ such that

$$C_1(t_r)\|\theta_r\|^2_{1,\Omega} \le \delta(k,t_r) + k\sum_{q=0}^{r} w_{rq}\ a\big((\lambda'(t_r,t_q),\mu'(t_r,t_q),\theta_q),\theta_r\big). \qquad (4.2.10)$$

To bound the right hand side of (4.2.10) we observe that

$$\begin{aligned}\int_\Omega \lambda'(x,t_r,t_q)\nabla\cdot\theta(x,t_q)\nabla\cdot\theta(x,t_r)\ dx &\le \int_\Omega |\lambda'(x,t_r,t_q)|\ |\nabla\cdot\theta(x,t_q)|\ |\nabla\cdot\theta(x,t_r)|\ dx \\ &\le C_{qr}(\lambda)\ \|\theta_q\|_{1,\Omega}\ \|\theta_r\|_{1,\Omega}, \qquad (4.2.11)\end{aligned}$$

and

$$\begin{aligned}\int_\Omega \mu'(x,t_r,t_q)\varepsilon_{ij}(\theta_q)\varepsilon_{ij}(\theta_r)\ dx &\le \int_\Omega |\mu'(x,t_r,t_q)|\ |\varepsilon_{ij}(\theta_q)|\ |\varepsilon_{ij}(\theta_r)|\ dx \\ &\le 9C_{qr}(\mu)\ \|\theta_q\|_{1,\Omega}\ \|\theta_r\|_{1,\Omega}. \qquad (4.2.12)\end{aligned}$$

where

$$\begin{aligned}0 < C_{qr}(\lambda) &:= \|\lambda'(x,t_r,t_q)\|_{0,\infty,\Omega}, \\ 0 < C_{qr}(\mu) &:= \|\mu'(x,t_r,t_q)\|_{0,\infty,\Omega}.\end{aligned}$$

The strict inequality is a consequence of assumption 2.1.1. Then combining (4.2.10-12) gives

$$\begin{aligned}C_1(t_r)\|\theta_r\|^2_{1,\Omega} &\le |\delta(k,t_r)| + k\|\theta_r\|_{1,\Omega}\sum_{q=0}^{r} w_{rq}\big(C_{qr}(\lambda) + 9C_{qr}(\mu)\big)\ \|\theta_q\|_{1,\Omega} \\ &\le |\delta(k,t_r)| + C_2(t_r)k\|\theta_r\|_{1,\Omega}\sum_{q=0}^{r}\|\theta_q\|_{1,\Omega}, \qquad (4.2.13)\end{aligned}$$

with

$$C_2(t_r) := \operatorname*{ess\ sup}_{0\le q\le r}\Big\{|w_{rq}|\ |C_{qr}(\lambda) + 9C_{qr}(\mu)|\Big\}. \qquad (4.2.14)$$

Turning to the quadrature error, δ, we see from (4.2.9) that

$$\begin{aligned}|\delta(k,t_r)| &\le |C_r|k^2\bigg(\Big|\int_\Omega \big(\lambda'(t_r,\tilde\tau)\nabla\cdot u^h(\tilde\tau)\big)''\nabla\cdot\theta_r\ dx\Big| + \Big|\int_\Omega \big(\mu'(t_r,\tilde\tau)\varepsilon_{ij}\big(u^h(\tilde\tau)\big)\big)''\varepsilon_{ij}(\theta_r)\ dx\Big|\bigg) \\ &\le |C_r|k^2\Big(\|\big(\lambda'(t_r,\tilde\tau)\nabla\cdot u^h(\tilde\tau)\big)''\|_{0,\Omega} + \|\big(\mu'(t_r,\tilde\tau)\varepsilon_{ij}\big(u^h(\tilde\tau)\big)\big)''\|_{0,\Omega}\Big)\ \|\theta_r\|_{1,\Omega} \\ &\le C_3(t_r,u^h)k^2\|\theta_r\|_{1,\Omega}. \qquad (4.2.15)\end{aligned}$$

Using this in (4.2.13) we have

$$C_1(t_r)\|\theta_r\|_{1,\Omega} \le C_3(t_r,u^h)k^2 + C_2(t_r)k\sum_{q=0}^{r}\|\theta_q\|_{1,\Omega}$$

or, for k small enough, by rearrangement this is

$$(C_1(t_r) - kC_2(t_r))\|\theta_r\|_{1,\Omega} \le C_3(t_r,u^h)k^2 + C_2(t_r)k\sum_{q=0}^{r-1}\|\theta_q\|_{1,\Omega},$$

therefore

$$\|\theta_r\|_{1,\Omega} \le C_5(u^h)k^2 + C_4k\sum_{q=0}^{r-1}\|\theta_q\|_{1,\Omega} \qquad \forall t_r \in \mathcal{I}^k, \tag{4.2.16}$$

where

$$C_4 := \operatorname*{ess\ sup}_{t\in\mathcal{I}} \frac{C_2(t)}{C_1(t)-kC_2(t)}, \quad C_5(u^h) := \operatorname*{ess\ sup}_{t\in\mathcal{I}} \frac{C_3(t,u^h)}{C_1(t)-kC_2(t)}.$$

We may now bring these results together and state the following theorem for the discrete problem $\mathbf{P}_1^{h,k}$:

Theorem 4.2.1. *If the conditions of theorem 3.2.1 are satisfied together with the additional requirements: i) $k < C_1(t)/C_2(t)$ $\forall t\in\mathcal{I}$, ii) assumption 2.2.1 is strengthened so that $g(x,\cdot)$, $f(x,\cdot)\in C^2(\mathcal{I})$. Then for the error associated with $\mathbf{P}_1^{h,k}$, the fully discrete approximation to $\mathbf{P}_1$: $\forall t_r \in \mathcal{I}^k$ $\exists C\ge 0$ depending upon $u(x,t)$ and $u^h(x,t)$ but independent of h and k such that*

$$\|u(x,t_r) - \left(u^h(x)\right)_r\|_{1,\Omega} \le C(h^\alpha + k^2) \qquad \forall t_r \in \mathcal{I}^k.$$

Proof. *Apply Gronwall's inequality (lemma 2.2.3) to (4.2.16) to give*

$$\|\theta_r\|_{1,\Omega} \le \hat{C}_5k^2\exp(\hat{C}_4t_I) \qquad \forall t_r\in\mathcal{I}^k,$$

where the ˆ denotes suprema over $\mathcal{I}$ of the appropriate quantity, and then combine this result with theorem 3.2.1 using (4.2.6) to obtain the desired result ∎

4.3 Full discretization of $\mathbf{P}_2$.

4.3.1 Full discretization.

With (4.2.2,3) still in force we obtain a fully discrete analogue of (3.3.3) by employing the following finite difference replacement [11]:

$$\int_{t_{i-1}}^{t_i}\gamma(\tau)u'(\tau)\,d\tau \approx \frac{\Delta U_i}{k_i}\int_{t_{i-1}}^{t_i}\gamma(\tau)\,d\tau, \tag{4.3.1}$$

where

$$\Delta U_i := U_i - U_{i-1}, \quad 1\le i\le I, \quad \text{with} \quad U_i(x)\approx u(x,t_i). \tag{4.3.2}$$

Applying this to (3.3.3) we obtain:

$\mathbf{P}_2^{h,k}$: Find $\left(u^h(x)\right)_j \in \mathcal{V}^h$ for each $t_j\in\mathcal{I}^k$ such that

$$\sum_{q=1}^{j}\frac{\Delta U_q}{k_q}\int_{t_{q-1}}^{t_q} A(t_j,\tau)\,d\tau = b_j, \quad 1\le j\le I, \tag{4.3.3}$$

with

$$U_0 = \left(A(0,0)\right)^{-1}F_0, \tag{4.3.4}$$

where (4.3.4) follows from (3.3.4). Rearranging (4.3.3) U_j is given explicitly in terms of known quantities. Note that this method of discretization corresponds closely to the midpoint rule for Volterra first kind integral equations which is known to have desirable convergence and stabilty properties [13]. The numerical results presented in §5 bear this observation out. Again we note that the method is not restricted to constant k as higher order methods, obtained by higher order finite difference approximations, would be.

4.3.2 Completion of the error estimate for $\mathbf{P}_2$.

We again use θ as defined in §4.2.2 and employ a constant time step k to provide a bound for θ_r in the norm $\|\cdot\|_{1,\Omega}$. We commence by evaluating (3.3.2) at $t = t_r \in \mathcal{I}^k$ and subtract (4.3.3) from this, giving

$$\sum_{q=1}^{r}\int_{t_{q-1}}^{t_q} a\big((\lambda(t_r,\tau),\mu(t_r,\tau),\chi_q),v^h\big)\,d\tau = 0 \qquad \forall v^h \in \mathcal{V}^h, \tag{4.3.5}$$

where

$$\chi_q := \big(u^h(x,\tau)\big)' - \frac{\Delta U_q}{k}, \qquad \tau \in (t_{q-1},t_q) \tag{4.3.6}$$

$$\Delta U_q := U_q - U_{q-1}. \tag{4.3.7}$$

Now, assuming sufficient smoothness with respect to time, we use Taylor's series about the mid-point of each time interval (t_{q-1},t_q). Specifically we assume $u(x,\cdot) \in \mathcal{C}^3(\mathcal{I})$ (i.e. we strengthen assumption 2.2.1 to: $f(x,\cdot),\ g(x,\cdot) \in \mathcal{C}^3(\mathcal{I})$.) and define for $1 \le q \le r$ and $\tau \in (t_{q-1},t_q)$

$$\delta(q,\tau) = \big(u^h(\tau)\big)' - \frac{\big(u^h(t_q) - u^h(t_{q-1})\big)}{k} \tag{4.3.8}$$

and note that Taylor's series with the Lagrange form of the remainder gives

$$\begin{aligned}\delta(q,\tau) &:= (\tau - c_q)\big(u^h(c_q)\big)'' + \frac{(\tau-c_q)^2}{2}\big(u^h(\alpha_{1,q}(\tau))\big)''' - \frac{k^2}{24}\big(u^h(\alpha_{2,q})\big)''' \\ c_q &:= (t_{q-1}+t_q)/2 \\ \alpha_{1,q}(\tau) &:= c_q + \omega(\tau - c_q) \qquad \text{for some } \omega \in (0,1) \\ \alpha_{2,q} &\in (t_{q-1},t_q).\end{aligned} \tag{4.3.9}$$

Hence, since $u^h(x,t_q) = U_q(x) + \theta_q$ the function χ_q is given by

$$\chi_q == \frac{\theta_q - \theta_{q-1}}{k} + \delta(q,\tau) \qquad \text{for } \tau \in (t_{q-1},t_q),\ 1 \le q \le r. \tag{4.3.10}$$

Now we choose $v^h = \big(\theta(x)\big)_r$ in (4.3.5) giving

$$\sum_{q=1}^{r}\int_{t_{q-1}}^{t_q} a\big((\lambda(t_r,\tau),\mu(t_r,\tau),(\theta_q-\theta_{q-1})/k + \delta(q,\tau)),\theta_r\big)\,d\tau = 0,$$

expanding the definition of $a\big((\lambda,\mu,\ \cdot\ ),\ \cdot\ \big)$ given by (2.2.7) we write this as

$$\begin{aligned}\frac{1}{k}\sum_{q=1}^{r}\int_\Omega \nabla\cdot(\theta_q-\theta_{q-1})\nabla\cdot\theta_r \int_{t_{q-1}}^{t_q}\lambda(t_r,\tau)\,d\tau + \varepsilon_{ij}(\theta_q-\theta_{q-1})\varepsilon_{ij}(\theta_r)\int_{t_{q-1}}^{t_q}\mu(t_r,\tau)\,d\tau\,dx \\ + \sum_{q=1}^{r}\int_{t_{q-1}}^{t_q} a\big((\lambda(t_r,\tau),\mu(t_r,\tau),\delta(q,\tau)),\theta_r\big)\,d\tau = 0.\end{aligned} \tag{4.3.11}$$

Rearranging the sum gives, equivalently

$$\begin{aligned}\frac{1}{k}\int_\Omega \nabla\cdot\theta_r\nabla\cdot\theta_r \int_{t_{r-1}}^{t_r}\lambda(t_r,\tau)\,d\tau + \varepsilon_{ij}(\theta_r)\varepsilon_{ij}(\theta_r)\int_{t_{r-1}}^{t_r}\mu(t_r,\tau)\,d\tau\,dx \\ + \frac{1}{k}\sum_{q=1}^{r-1}\int_\Omega \nabla\cdot\theta_r\nabla\cdot\theta_q\Big[\int_{t_{q-1}}^{t_q}\lambda(t_r,\tau)\,d\tau - \int_{t_q}^{t_{q+1}}\lambda(t_r,\tau)\,d\tau\Big]\,dx \\ + \frac{1}{k}\sum_{q=1}^{r-1}\int_\Omega \varepsilon_{ij}(\theta_r)\varepsilon_{ij}(\theta_q)\Big[\int_{t_{q-1}}^{t_q}\mu(t_r,\tau)\,d\tau - \int_{t_q}^{t_{q+1}}\mu(t_r,\tau)\,d\tau\Big]\,dx \\ + \sum_{q=1}^{r}\int_{t_{q-1}}^{t_q} a\big((\lambda(t_r,\tau),\mu(t_r,\tau),\delta(q,\tau)),\theta_r\big)\,d\tau = 0.\end{aligned} \tag{4.3.12}$$

Due to the fact that λ and μ may be assumed continuous in time (assumptions 2.1.1) this may be rewritten, by liberally applying the mean value theorem, as

$$\int_\Omega \lambda(t_r,\bar\tau_{1r})\ \nabla\cdot\theta_r\nabla\cdot\theta_r + \mu(t_r,\bar\tau_{2r})\varepsilon_{ij}(\theta_r)\varepsilon_{ij}(\theta_r)\ dx$$
$$- C_k k\sum_{q=1}^{r-1}\int_\Omega \lambda'(t_r,\tilde\tau_{1rq})\nabla\cdot\theta_r\nabla\cdot\theta_q + \mu'(t_r,\tilde\tau_{2rq})\varepsilon_{ij}(\theta_r)\varepsilon_{ij}(\theta_q)\ dx$$
$$+ \sum_{q=1}^{r}\int_{t_{q-1}}^{t_q} a\big((\lambda(t_r,\tau),\mu(t_r,\tau),\delta(q,\tau)),\theta_r\big)\ d\tau = 0, \qquad (4.3.13)$$

where $0 \le C_k \le 2$. Now, $\lambda(t_r,\bar\tau_{1r})$, $\mu(t_r,\bar\tau_{2r}) > 0$ by assumption 2.1.1, so observing remark 2.2.1 $\exists C_1(t_r) > 0$ such that

$$C_1(t_r)\|\theta_r\|_{1,\Omega}^2 \le C_k k\sum_{q=1}^{r-1}\int_\Omega \lambda'(t_r,\tilde\tau_{1rq})\nabla\cdot\theta_r\nabla\cdot\theta_q + \mu'(t_r,\tilde\tau_{2rq})\varepsilon_{ij}(\theta_r)\varepsilon_{ij}(\theta_q)\ dx$$
$$- \sum_{q=1}^{r}\int_{t_{q-1}}^{t_q} a\big((\lambda(t_r,\tau),\mu(t_r,\tau),\delta(q,\tau)),\theta_r\big)\ d\tau. \qquad (4.3.14)$$

Taking absolute values we express (4.3.14) as

$$C_1(t_r)\|\theta_r\|_{1,\Omega}^2 \le C_k k\sum_{q=1}^{r-1}\|\theta_q\|_{1,\Omega}\|\theta_r\|_{1,\Omega}\big(|\hat\lambda'(t_r,\tilde\tau_{1rq})| + 9|\hat\mu'(t_r,\tilde\tau_{2rq})|\big)$$
$$+ \sum_{q=1}^{r}\left|\int_{t_{q-1}}^{t_q} a\big((\lambda(t_r,\tau),\mu(t_r,\tau),\delta(q,\tau)),\theta_r\big)\ d\tau\right|. \qquad (4.3.15)$$

Turning now to the term involving the truncation error δ. We note that from (4.3.9),

$$\int_{t_{q-1}}^{t_q} a\big((\lambda(t_r,\tau),\mu(t_r,\tau),\delta(q,\tau)),\theta_r\big)\ d\tau = \int_{t_{q-1}}^{t_q} a\big((\lambda(t_r,\tau),\mu(t_r,\tau),\overline{\delta}(q,\tau)),\theta_r\big)\ d\tau \qquad (4.3.16)$$

where

$$\overline{\delta}(q,\tau) := \frac{(\tau-c_q)^2}{2}\big(u^h(\alpha_{1,q}(\tau))\big)''' - \frac{k^2}{24}\big(u^h(\alpha_{2,q})\big)''' \qquad (4.3.17)$$

as a consequence of the elementary result

$$\int_{t_{q-1}}^{t_q}(\tau - c_q)d\tau = 0. \qquad (4.3.18)$$

Thus we have for each component of the sum in (4.3.15)

$$\left|\int_{t_{q-1}}^{t_q} a\big((\lambda(t_r,\tau),\mu(t_r,\tau),\delta(q,\tau)),\theta_r\big)\ d\tau\right|$$
$$\le \left.\int_\Omega |\nabla\cdot\theta_r|\int_{t_{q-1}}^{t_q}|\lambda(t_r,\tau)|\ |\nabla\cdot\overline{\delta}(q,\tau)|\ d\tau dx + \int_\Omega |\varepsilon_{ij}(\theta_r)|\int_{t_{q-1}}^{t_q}|\mu(t_r,\tau)|\ |\varepsilon_{ij}\big(\overline{\delta}(q,\tau)\big)|\ d\tau dx\right|$$
$$\le k|\hat\lambda(t_r,\tilde\tau_q)|\int_\Omega|\nabla\cdot\theta_r|\ |\nabla\cdot\overline{\delta}(q,\tilde\tau_q)|\ dx + k|\hat\mu(t_r,\bar\tau_q)|\int_\Omega|\varepsilon_{ij}(\theta_r)|\ |\varepsilon_{ij}\big(\overline{\delta}(q,\bar\tau_q)\big)|\ dx$$
$$\le k|\hat\lambda(t_r,\tilde\tau_q)|\ \|\theta_r\|_{1,\Omega}\|\overline{\delta}(q,\tilde\tau_q)\|_{1,\Omega} + k|\hat\mu(t_r,\bar\tau_q)|\ \|\theta_r\|_{1,\Omega}\|\overline{\delta}(q,\bar\tau_q)\|_{1,\Omega}, \qquad (4.3.19)$$

From (4.3.17) we have the bound

$$\|\overline{\delta}(q,\tilde\tau)\|_{1,\Omega},\ \|\overline{\delta}(q,\bar\tau)\|_{1,\Omega} \le C_{\overline{\delta}}k^2 \qquad \forall\tau\in\mathcal{I} \qquad (4.3.20)$$

Now if we take appropriate suprema over the interval $[t_0, t_r]$ we may write (4.3.15) as

$$\|\theta_r\|_{1,\Omega} \leq C_2 t_I k^2 + C_3 k \sum_{q=1}^{r-1} \|\theta_q\|_{1,\Omega} \qquad \forall t_r \in \mathcal{I}^k. \tag{4.3.21}$$

Hence we have the following

Theorem 4.3.1. *If the conditions required by theorem 3.3.1 are satisfied and further if assumption 2.2.1 is strengthened to $f(x,\cdot)$, $g(x,\cdot) \in \mathcal{C}^3(\mathcal{I})$ then for the error associated with $\mathbf{P}_2^{h,k}$, the fully discrete approximation to $\mathbf{P}_2$, $\forall t_r \in \mathcal{I}^k$ $\exists C \geq 0$ depending upon $u^h(x,t)$ but not on h and k such that*

$$\|u(x,t_r) - \left(u^h(x)\right)_r\|_{1,\Omega} \leq C(h^\alpha + k^2) \qquad \forall t_r \in \mathcal{I}^k.$$

Proof. *Apply lemma 2.2.3 to (4.3.21) to obtain*

$$\|\theta_r\|_{1,\Omega} \leq C_2 t_I k^2 \exp(C_3 t_I) \qquad \forall t_r \in \mathcal{I}^k,$$

and use (4.2.6) in the context of $\mathbf{P}_2^{h,k}$. ∎

5 Numerical experiments.

5.1 Preamble.

In this final section we predicate the theoretical convergence rates given in theorems 4.2.1 and 4.3.1 by computing the approximate solution to simple model problems for which the analytical solutions are known. These solutions are found via the correspondence principle [4], which enables the viscoelastic solution to be derived from the corresponding linear elastic solution by using integral transform techniques. The correspondence principle is only applicable to non-ageing materials. Accordingly we set, neglecting the x dependence,

$$\lambda(t,\tau) = \lambda(t-\tau), \tag{5.1.1}$$
$$\mu(t,\tau) = \mu(t-\tau). \tag{5.1.2}$$

We shall assume that the time dependent part of λ and μ may be modelled adequately by expressions of the form:

$$\varphi(t) = \sum_{i=0}^{N} C_i e^{-\alpha_i t}, \tag{5.1.3}$$

which are suggested by the appearance of stress relaxation curves for real viscoelastic materials, see the data for "Maranyl"[2] in §5.4 for example, or the curves given in [1]. This form for λ and μ introduces an important simplification into the numerical algorithms (4.2.5) and (4.3.3). Usually in solving these kinds of integral equation problems the solutions obtained at each time step up until the current one must be stored in order to compute the history integral. This can be very demanding on computational storage. However, for history kernels of the form (5.1.3) and for $\mathbf{P}_2^{h,k}$ we exploit the relation:

$$\int_0^{t_i} e^{-\alpha_i(t_i-\tau)} g(\tau)\, d\tau = e^{-\alpha_i(t_i - t_{i-1})} \int_0^{t_{i-1}} e^{-\alpha_i(t_{i-1}-\tau)} g(\tau)\, d\tau + \int_{t_{i-1}}^{t_i} e^{-\alpha_i(t_i-\tau)} g(\tau)\, d\tau \tag{5.1.4}$$

for any function g, i.e. for each term of the sum in (5.1.3) the history integral at time t_j may be obtained simply by attenuating the result at the previous time, t_{j-1}, by an amount dependent upon the current time step. Thus only $N+1$ solution vectors, per viscoelastic function, need be stored in order to evaluate the history term completely, see [11]. A similar observation can be made for $\mathbf{P}_1^{h,k}$

In the final subsection we compare the numerically computed results with the experimental stress relaxation and creep data for a real engineering material [2], which we assume to be non-ageing. Also, following the manufacturer's recommendations we take $\lambda(t) \propto \mu(t)$, the constant of proportionality being obtained from the linear elastic definitions of the Lamé coefficients, which are given usually in terms of Young's modulus and the Poisson ratio, the latter of which will be constant when this proportionality exists between the viscoelastic functions and the former is embodied in the relaxation functions themselves.

5.2 Benchmark analytical solutions.

5.2.1 Linear elastic solutions.

For the problem (2.2.1,. . .,3) we take $n = 2$ and define the domain Ω to be the rectangle

$$\Omega := \{x, y \in \mathcal{R} : \ 0 < x < l, \ 0 < y < 2k, \ l, k > 0\}, \tag{5.2.1}$$

and present two linear elastic solutions to the problems arising when Ω has certain body forces and surface tractions imposed over it and on it (resp.). (Although l and k have been used in previous sections with quite different meanings, the usage in (5.2.1) is essentially confined to this section (5.2), definite values of l and k, in this sense, being assigned in all the following work.) The first of these solutions has displacements that vary quadratically in x and y, so that if the finite element employed in the computation is composed of quadratic basis functions the spatial behavior of the displacements may be captured exactly by the numerical scheme thus isolating the time discretization error. The second solution is completely artificial in that the body forces are dependent on the Poisson ratio of the material, for our purposes this is immaterial since we are interested only in the behaviour of the numerical solution, the displacements arising in this case are sinusoidal. The domain Ω is shown schematically in figure 5.2.1, where, in the previous notation

$$(x, y) := (x_1, x_2), \tag{5.2.2}$$

$$(u_E, v_E) := (u_1, u_2), \tag{5.2.3}$$

$$(X, Y) := (f_1, f_2). \tag{5.2.4}$$

The subscript E denotes linear elastic solutions. When this subscript is dropped in §§5.2.2,3 the solutions will be for the corresponding linear viscoelastic solution.

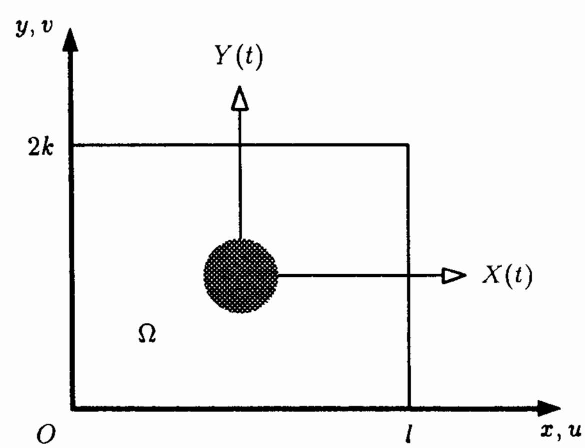

Figure 5.2.1

i) Quadratic solution.

To obtain a quadratic variation of displacement we impose upon Ω the following boundary conditions

$$u_E(0, k) = v_E(0, k) = v_E(l, k) = 0, \tag{5.2.5}$$

and assume that a spatially constant body force, $X(t)$, acts whilst $Y(t) \equiv 0$. Then we have the single non-zero surface traction:

$$g_1 = lX(t) \qquad \forall (x, y) \in \{x = 0, \ 0 < y < 2k\}. \tag{5.2.6}$$

Under these conditions the solution to (2.2.1) under the assumption of plane stress is given by

$$u_E(x,y,t) = \frac{X(t)}{2E}\left[(2lx - x^2) - \nu(y-k)^2\right], \tag{5.2.7}$$

$$v_E(x,y,t) = \frac{\nu X(t)}{E}(x-l)(y-k), \tag{5.2.8}$$

$$\sigma_{11} = X(t)\ (l-x), \tag{5.2.9}$$

$$\sigma_{12} = \sigma_{22} = 0. \tag{5.2.10}$$

Rotating Ω through 90° clockwise we see that this problem corresponds to the physical situation of a plate suspended from the midpoint of its uppermost edge and deflecting vertically under the action of its own weight. In these expressions E is the Young's modulus of the material and $\nu < 1/2$ the Poisson ratio.

ii) Trigonometric solution.

As remarked above, this is an artificial solution because the body forces depend upon the Poisson ratio of the material. We set

$$X(t) = \frac{\phi(\nu+1)N(t)}{(\nu-1)}\cos\phi x + \xi^2 x L(t)\sin\xi(y-1/2), \tag{5.2.11}$$

$$Y(t) = \frac{\xi(\nu+1)L(t)}{(\nu-1)}\cos\xi(y-1/2) + \phi^2(y-1/2)N(t)\sin\phi x, \tag{5.2.12}$$

and employ the essential boundary condition (5.2.5). Under the assumption of plane stress it can be shown that the solution of (2.2.1) is now given by

$$u_E(x,y,t) = \frac{2(1+\nu)L(t)}{E}x\sin\xi(y-1/2), \tag{5.2.13}$$

$$v_E(x,y,t) = \frac{2(1+\nu)N(t)}{E}(y-1/2)\sin\phi x, \tag{5.2.14}$$

$$\sigma_{11}(x,y,t) = \frac{2}{(1-\nu)}\left[L(t)\sin\xi(y-1/2) + \nu N(t)\sin\phi x\right], \tag{5.2.15}$$

$$\sigma_{22}(x,y,t) = \frac{2}{(1-\nu)}\left[N(t)\sin\phi x + \nu L(t)\sin\xi(y-1/2)\right], \tag{5.2.16}$$

$$\sigma_{12}(x,y,t) = \xi x L(t)\cos\xi(y-1/2) + \phi(y-1/2)N(t)\cos\phi x, \tag{5.2.17}$$

when the tractions are applied consistent with these expressions for σ_{ij}.

5.2.2 Linear viscoelastic solutions (non-ageing).

Linear viscoelastic solutions for non-ageing materials may be generated from particular types of linear elastic solutions via the correspondence principle [3,4]. To give a simple example of how this may be achieved we firstly assume that the time dependent parts of λ and μ are proportional, i.e.

$$\lambda(t) \propto \mu(t), \tag{5.2.18}$$

this is tantamount to assuming a constant Poisson ratio. In terms of the D matrix of (2.1.12) or (2.1.13) this means that we have, omitting again the dependence on x, the representation

$$D(t) = D_0\varphi(t), \tag{5.2.19}$$

where D_0 is a constant matrix. Thus we have the relation

$$\sigma(t) = \int_{0-}^{t} D_0\vartheta(t-\tau)\varepsilon(\tau)\,d\tau, \quad \vartheta(t) := \frac{\partial}{\partial t}\left[H(t)\varphi(t)\right], \tag{5.2.20}$$

where $H(t)$ is the Heaviside step function. The function $\varphi(t)$ represents the time dependent behaviour of λ, and therefore of μ also, the constant of proportionality being embodied in the matrix D_0. Now taking, for example, the Laplace transform of (5.2.20) which is of the convolution form we have

$$\hat{\sigma}(s) = D_0\hat{\vartheta}(s)\hat{\varepsilon}(s). \tag{5.2.21}$$

Notice that any spatial variation of these quantities is unaffected by this operation.

Also, suppose that we know a linear elastic solution expressed in the form

$$\sigma_E(x) = D_E\varepsilon_E(x) \tag{5.2.22}$$

which is time independent. The correspondence principle may now be invoked; this consists of replacing D_E in (5.2.22) by $D_0\hat{\vartheta}(s)$ and treating σ_E and ε_E as $\hat{\sigma}(s)$ and $\hat{\varepsilon}(s)$ respectively. The result may then be transformed inversely to yield the viscoelastic solution corresponding to (5.2.22). Obviously, if the quantities in (5.2.22) are time dependent this must be incorporated in the transformation-replacement-inversion procedure.

We consider the simple case where the body forces $X(t)$ and $Y(t)$ are expressed in terms of the single function

$$p(t) = a_1 + e^{-\beta t}(a_2 \sin\omega t + a_3\cos\omega t) \tag{5.2.23}$$

$$\Rightarrow \qquad \hat{p}(s) = \frac{a_1}{s} + \frac{a_2\omega + a_3(s+\beta)}{(s+\beta)^2+\omega^2}, \tag{5.2.24}$$

In the first example we assume that $X(t) = p(t)$ and in the second example we assume that $X(t)$ and $Y(t)$ are given by (5.2.11-12) with $L(t) = Lp(t)$ and $N(t) = Np(t)$ where L and N do not vary with time.

For simplicity we take the stress relaxation function $\varphi(t)$ of the form (5.1.3) but with only 2 terms, i.e.

$$\varphi(t) = C_0 + C_1e^{-bt}, \quad C_0, C_1, b > 0, \tag{5.2.25}$$

$$\Rightarrow \hat{\varphi}(s) = g_0 + \frac{g_1}{s+b}, \quad Re(b) < Re(s), \tag{5.2.26}$$

where

$$g_0 := C_0 + C_1 > 0,$$
$$g_1 := -bC_1 < 0.$$

Performing the replacement-inversion procedure indicated earlier we find that for $u_E(x,y,t)$ and $v_E(x,y,t)$ given by either the quadratic or sinusoidal solution

$$\begin{aligned}\frac{u(x,y,t)}{u_E(x,y,t)} = \frac{v(x,y,t)}{v_E(x,y,t)} = &\frac{a_1(bg_0+g_1e^{-ht})}{g_0(bg_0+g_1)} \\ &+ \frac{1}{g_0((h-\beta)^2+\omega^2)}\Big[(b-h)\big(a_2\omega + a_3(\beta-h)\big)e^{-ht} \\ &+ e^{-\beta t}\big((h-\beta)(b-\beta)+\omega^2\big)(a_2\sin\omega t + a_3\cos\omega t) \\ &+ e^{-\beta t}\omega(b-h)(a_3\sin\omega t - a_2\cos\omega t)\Big],\end{aligned} \tag{5.2.27}$$

where

$$h := \frac{bg_0+g_1}{g_0}. \tag{5.2.28}$$

Expression (5.2.27) furnishes us with the exact solution to the corresponding linear, non-ageing viscoelastic problem.

5.2.3 Viscoelastic Poisson effect.

In more general cases the assumption of constant Poisson ratio embodied in (5.2.18) will not be appropriate. In this case we must assume that the time dependent behaviour of λ and μ will be uncorrelated and a deformed body may therefore exhibit a viscoelastic Poisson effect, i.e. a time dependent Poisson ratio.

Again using correspondence principles, this time under the assumption of plane strain we present an analytical solution to a very simple problem which exhibits this time dependent Poisson effect. We use Ω as defined by (5.2.1), with $l = 1$ and $k = 1/2$ and impose the essential boundary condition

$$\begin{aligned} u_E(0,y) = 0, \qquad u_E(1,y) = \ell > 0 \text{ (and constant)} \ \ \forall y \in [0,1] \\ v_E(x,1/2) = 0 \ \forall x \in [0,1], \end{aligned} \tag{5.2.29}$$

and assume zero tractions over $(x,y) \in \{0 < x < 1;\ y = 0,1\}$ and identically zero body forces. Note that the boundary condition (2.2.2) is violated by this. In this case the linear elastic solution is given by

$$\begin{aligned} \varepsilon_{11} &= \ell, \\ \varepsilon_{22} &= -\frac{\nu\ell}{1-\nu}. \end{aligned} \tag{5.2.30}$$

We may relate the Poisson ratio to the bulk modulus, K, and the shear modulus, G, by the relations (2.1.5). Specifically we have

$$\nu = \frac{3K - 2G}{6K + 2G} \tag{5.2.31}$$

and define the Lamé coefficients via

$$\begin{aligned} \mu &= 2G \\ \lambda &= K - \frac{1}{3}\mu. \end{aligned} \tag{5.2.32}$$

To determine the corresponding viscoelastic solution we assume the forms

$$K(t) = K_0 \exp(-k_0 t) \tag{5.2.33}$$

and

$$G(t) = G_0 \exp(-g_0 t) \tag{5.2.34}$$

for the viscoelastic bulk and shear moduli, (the assumptions 2.1.1 are satisfied). Thinking again of the transformation-replacement procedure outlined above, we have, in the transform domain,

$$\hat{\nu}(s) = \frac{3K_0(s+g_0) - 2G_0(s+k_0)}{6K_0(s+g_0) + 2G_0(s+k_0)} \tag{5.2.35}$$

and thus, since ℓ is a constant:

with

$$\begin{aligned} A &= -\ell(3K_0 - 2G_0), \qquad & B &= -\ell(3K_0 g_0 - 2G_0 k_0), \\ C &= 3K_0 + 4G_0, \qquad & D &= 3K_0 g_0 + 4G_0 k_0, \end{aligned}$$

we may write

$$\begin{aligned} \hat{\varepsilon}_{22}(s) &= \frac{(B/D)}{s} + \frac{(A/C) - (B/D)}{s + (D/C)} \\ \Rightarrow \varepsilon_{22}(t) &= \ell\nu(t) \end{aligned} \tag{5.2.36}$$

where

$$\nu(t) = N_0 + N_1 \exp(-Nt) \tag{5.2.37}$$

and

$$\begin{aligned} N_0 &= -\frac{3K_0 g_0 - 2G_0 k_0}{3K_0 g_0 + 4G_0 k_0} \\ N_1 &= \frac{3K_0 g_0 - 2G_0 k_0}{3K_0 g_0 + 4G_0 k_0} - \frac{3K_0 - 2G_0}{3K_0 + 4G_0} \\ N &= \frac{3K_0 + 4G_0}{3K_0 g_0 + 4G_0 k_0}. \end{aligned}$$

We may think of $\nu(t)$ as a manifestation of the viscoelastic Poisson ratio under plane strain, note that $g_0 = k_0 \Rightarrow \epsilon_{22}(0) = \epsilon_{22}(\infty)$ because $N_1 = 0$, which is exactly the case when it is assumed that $\lambda \propto \mu$, i.e., the Poisson ratio is constant.

5.3 Numerical results.

In this section we shall give graphical indication of the performance of the algorithms $\mathbf{P}_1^{h,k}$ and $\mathbf{P}_2^{h,k}$ by solving numerically the test problems developed in the foregoing sections. For this we take, in (5.2.1), $(l, 2k) = (1, 1)$. Also, rather than calculate $\|u(x, t_r) - (u^h(x))_r\|_{1,\Omega}$ to verify theorems 4.2.1 and 4.3.1 we calculate the more interesting quantity $\|\sigma(x, t_r) - (\sigma^h(x))_r\|_{0,\Omega}$, which we may reasonably expect to be bounded in the same way because the stress, σ, depends upon the space derivatives of u.

In common with the standard practice of computational finite element implementation we shall perform all spatial integrations on a reference element using a sufficiently high order quadrature rule. Also we take the standard 8-noded quadrilateral finite element, in which case the basis functions on this reference element are of the form $\sum_{i,j=0}^{2} \alpha_{ij} x^i y^j$, where $\alpha_{22} \equiv 0$. The domain is partioned into squares of side length h such that h^{-1} is an integer. Also, for simplicity, we take constant time step k.

In order to determine the order of convergence (i.e. the powers of h and k) suggested by the numerical performance of the algorithms we define β through

$$\beta := \frac{\log|e_{2h,2k}| - \log|e_{h,k}|}{\log 2}, \tag{5.3.1}$$

where $e_{h,k}$ is some numerically determined measure of the error resulting from the discretization, i.e. β is the indicated order of convergence of the scheme.

For all of the problems considered we assume the time dependent part of the body forces (5.2.23) to take the form:

$$p(t) = 1 + \exp(-\frac{1}{4}t)\ \sin\frac{\pi}{2}t. \tag{5.3.2}$$

Also, for the case of constant Poisson ratio we shall assume that $\nu = 0.4$ and in (5.2.25)

$$\varphi(t) = 1 + \exp(-2t), \tag{5.3.3}$$

whilst for the variable Poisson ratio example given in §5.2.3 we shall take for (5.2.33,34)

$$K(t) = 8\exp(-0.1t), \tag{5.3.4}$$
$$G(t) = 4.5\exp(-0.2t). \tag{5.3.5}$$

We emphasise that the values taken for the material functions are purely arbitrary, more realistic values are considered in the next section. Also, in order to present the graphical results in a clear manner the solutions obtained at each time level have been interpolated to produce continuous curves.

At the end of §4.3.1 we remarked that the numerical performance of $\mathbf{P}_2^{h,k}$ seems to indicate stability, in fact it appears that if the body forces and tractions tend to functions of the space variables alone, then for the type of relaxation function given by (5.3.3) the error due to the time discretization appears to vanish, leaving only the error due to the spatial discretization. This behaviour does not occur for $\mathbf{P}_1^{h,k}$. Figures 5.3.1,3 illustrate this by showing how the particular error, $e\big((1,\frac{1}{2}), t_r\big) := u_1\big((1,\frac{1}{2}), t_r)\big) - \big(u_1^h(1,\frac{1}{2})\big)_r$ varies through time. Also by taking $e_{h,k}$ to be $\|u - u^h\|_\infty$ (the maximum norm on $\mathcal{R}^n$) when applied to the nodal solution vector for two computations having time steps k and $2k$ we show in figures 5.3.2,4 the numerically suggested nodal convergence rate, β, for the displacements. For these calculations we have used the quadratic solution $(5.2.7, \ldots, 10)$ in which case we expect the finite element to capture the spatial behaviour exactly.

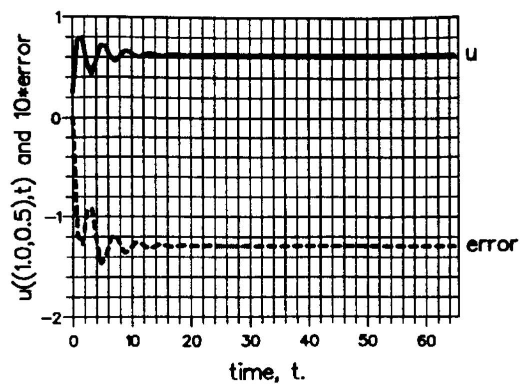

Figure 5.3.1 Algorithm $\mathbf{P}_1^{1,0.8}$, the computed solution for $\left(u_1^h(1,\frac{1}{2})\right)_r$ and the associated error. The discretization error tends to a constant as the body force tends to a function of x only.

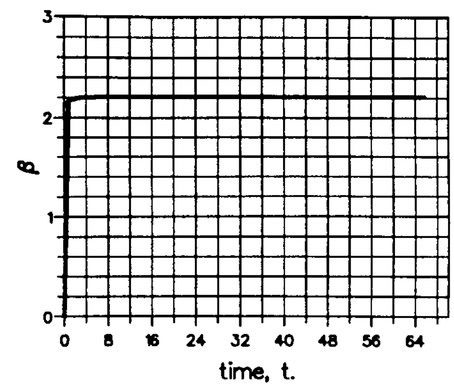

Figure 5.3.2 Algorithm $\mathbf{P}_1^{1,k}$, the estimated nodal convergence rate of the displacements with β, given by (5.3.1), obtained by considering $k = 0.8$ and $k = 0.4$.

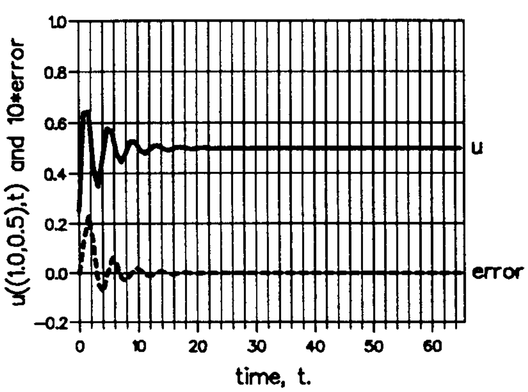

Figure 5.3.3 Algorithm $\mathbf{P}_2^{1,0.8}$, the computed solution for $\left(u_1^h(1,\frac{1}{2})\right)_r$ and the associated error. The discretization error tends to zero as the body force tends to a function of x only.

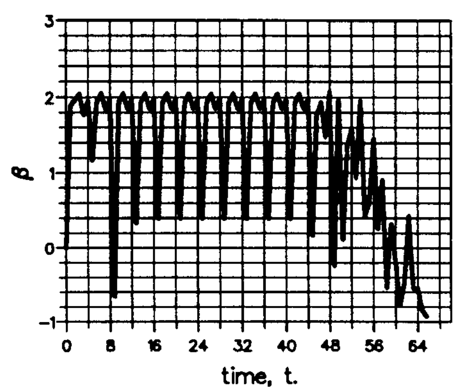

Figure 5.3.4 Algorithm $\mathbf{P}_2^{1,k}$, the estimated nodal convergence rate of the displacements with β, given by (5.3.1), obtained by considering $k = 0.8$ and $k = 0.4$.

Turning now to the trigonometric solution (5.2.13, ..., 17) with $\xi = \phi = \pi$ and $L(t)$, $N(t)$ given by (5.3.2) above, figures 5.3.5, ..., 8 show the variation of $\|\sigma - \sigma^h\|_{0,\Omega}$ with time and the numerically suggested convergence rate for the two cases $k \ll h$ and $h \ll k$. In each case the scheme appears to be $\mathcal{O}(h^2 + k^2)$ as expected. The integral involved in the calculation of $\|\cdot\|_{0,\Omega}$ was calculated numerically with an $\mathcal{O}(h^4)$ quadrature rule.

Finally, in figures 5.3.9,10 we show the numerically predicted viscoelastic Poisson effect. The caption to figure 5.3.9 shows the values assumed for the quantities defined in §5.2.3, and the figure itself shows the displacement u_2 at the point (1,1), i.e. the top right hand corner of the domain. The accompanying figure, 5.3.10, shows for interest only the apparent convergence rate of the strain at this point.

5.4 Comparison with a real material.

In [2] design data for the I.C.I. structural nylon 66 "Maranyl"(registered trade mark), type A101 is given. Specifically we refer to figures 1 and 3 contained therein. Figure 3 shows graphically the response of a test piece to a constant imposed axial strain by plotting the isometric axial stress *vs.* time curves for percentage strains of 0.5, 1.0, ..., 3.0, 3.5 under dry conditions at 20°C. Figure 1 shows the tensile creep behaviour resulting from constant imposed axial stresses of 500, 1000, ..., 7000, 7500 p.s.i. (pounds per square inch). Thus figures 1 and 3 represent collections of axial creep and axial stress relaxation curves respectively. Following the manufacturers recommendation we adopt a constant Poisson ratio of 0.4.

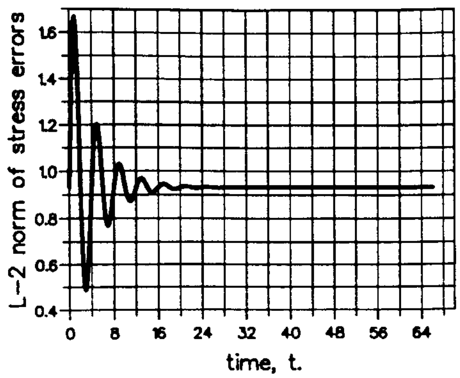

Figure 5.3.5 Algorithm $\mathbf{P}_1^{1,0.1}$, the computed value of $\|\sigma - \sigma^h\|_{0,\Omega}$. The discretization error tends to a constant as the body force tends to a function of x only.

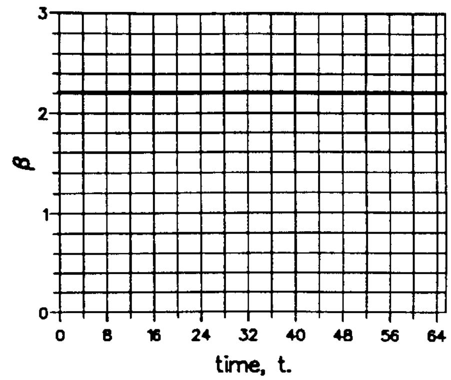

Figure 5.3.6 Algorithm $\mathbf{P}_1^{h,k}$, the estimated convergence rate of $\|\sigma - \sigma^h\|_{0,\Omega}$ with β, given by (5.3.1), obtained by considering $h = 1, k = 0.1$ and $h = 0.5.k = 0.05$.

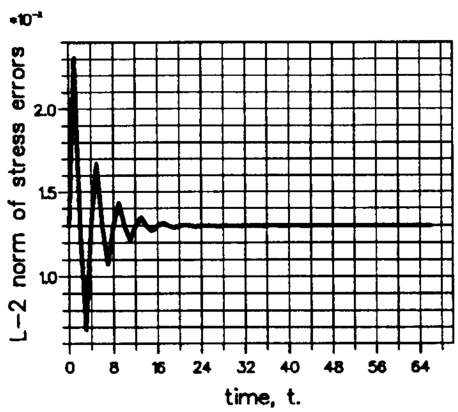

Figure 5.3.7 Algorithm $\mathbf{P}_1^{\frac{1}{8},1.0}$, the computed value of $\|\sigma - \sigma^h\|_{0,\Omega}$. The discretization error tends to a constant as the body force tends to a function of x only.

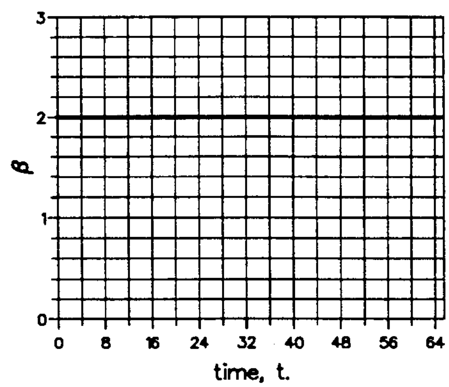

Figure 5.3.8 Algorithm $\mathbf{P}_1^{h,k}$, the estimated convergence rate of $\|\sigma - \sigma^h\|_{0,\Omega}$ with β, given by (5.3.1), obtained by considering $h = \frac{1}{8}, k = 1.0$ and $h = \frac{1}{16}, k = 0.5$.

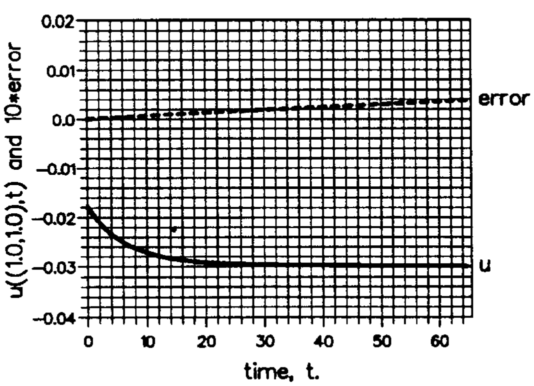

Figure 5.3.9 Algorithm $\mathbf{P}_1^{1.0,0.8}$, the computed value of $\varepsilon_{22}^h\big((u^h(1,1))_r\big)$ and the associated error, demonstrating the viscoelastic Poisson effect discussed in §5.2.3, in the notation of *that section* we have: $\ell = 0.1$, $K_0 = 8$, $k_0 = 0.1$, $G_0 = 4.5$ and $g_0 = 0.2$.

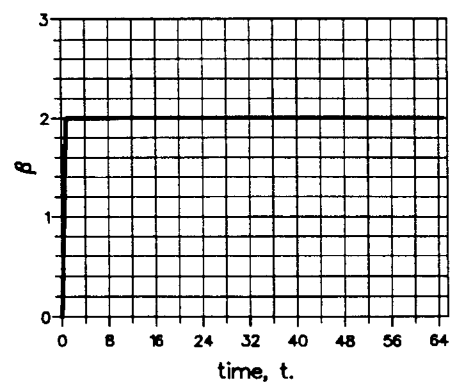

Figure 5.3.10 Algorithm $\mathbf{P}_1^{1,k}$, the estimated nodal convergence rate of $\varepsilon_{22} - \varepsilon_{22}^h$ at (1,1) with β, given by (5.3.1), obtained by considering $k = 0.8$ and $k = 0.4$.

In this section we use the 0.5% strain curve of figure 3 to calculate an axial stress relaxation function of the form (5.1.3) by using a least squares curve fitting routine (routine E04GEF of the NAG FORTRAN library, mk14). This obviously involves non-linear minimisation and therefore different minimising functions may result from different starting points, we found the following coefficients to represent the stress relaxation at 0.5% strain adequate:

$$\begin{aligned} C_0 &= 73\ 855.4 & \alpha_0 &= 0.0 \\ C_1 &= 155\ 338.4 & \alpha_1 &= 0.006\ 139\ 77 \\ C_2 &= 173\ 441.6 & \alpha_2 &= 0.000\ 181\ 719 \end{aligned} \tag{5.4.1}$$

Where the units of the C_i are p.s.i, and the α_i are $(\text{hours})^{-1}$.

The aim in this section is to test the predictive power of the numerical schemes by using this relaxation function to predict the creep curves given in figure 1 of [2] (in fact for brevity we use $\mathbf{P}_1^{h,k}$ only). The resulting behaviour is shown in figure 5.4.1. Here the data given in [2] has been reproduced in part by plotting the piecewise linear interpolate to selected points of figure 1, these are the solid lines. The calculations were performed under the assumption of plane stress.

The numerically computed results are based on a unit square domain discretized using a single 8-noded quadrilateral element as in §5.3 with the algorithm $\mathbf{P}_1^{1,2}$, i.e the time step is 2 hours, except for the first few steps where $k = 0.001$ to capture the short timescale behaviour. It can be seen that at low stresses the algorithm performs well but the deterioration of accuracy becomes very marked as the stress levels are increased. We conclude that the viscoelastic relationships implied by figures 1 and 3 of [2] are more complicated than we have allowed for, indeed it is most likely that the relationship will be non-linear in some way. The extension to non-linearity can occur in two independent ways: firstly the assumption of infinitesimal strain (2.1.3) may be replaced by some finite strain measure, secondly, the linear constitutive relationships (2.1.15,16) may be replaced by some more general form. Obviously the conjunction of these possibilities gives the most general case. Knauss and Emri [15] give an empirically determined formulation of non-linear viscoelasticity (also discussed in [16]) based on considering the free volume of the material which is used to define a reduced time, in this case the infinitesimal strain assumption is retained. However, the formulation of the more general problem consistent with the requirements of continuum mechanics has, to our knowledge, not yet been acheived [17].

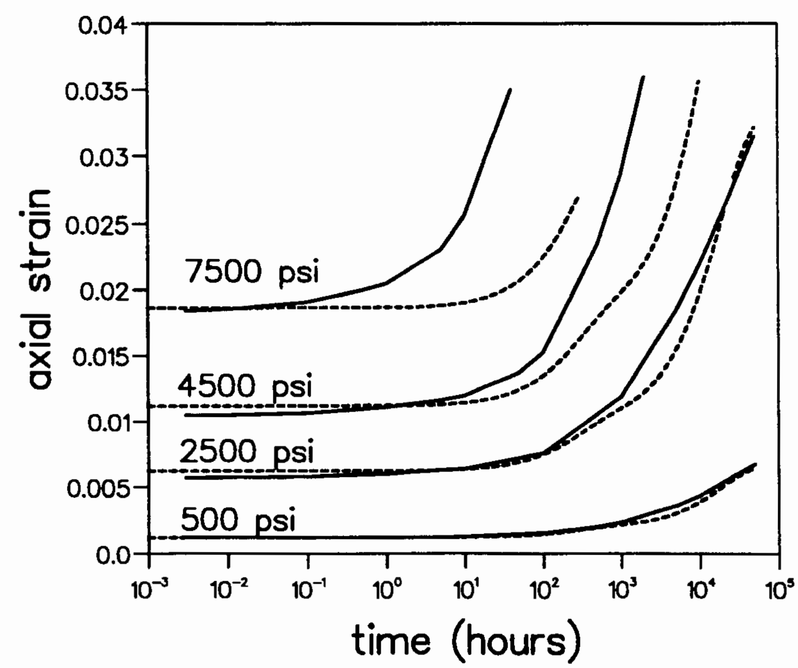

Figure 5.4.1

6 References.

[1] **Ferry, J. D.**, *Viscoelastic Properties of Polymers*, John Wiley & Sons. inc., third edition, 1980.

[2]**"Maranyl" nylon**, *Technical Service Note N 109*, Moulding Powders Group, I.C.I. Plastics Division, Welwyn Garden City, Herts, U.K.

[3] **Christensen, R. M.**, *Theory of Viscoelasticity, an Introduction*, Academic Press, London, 1971.

[4] **Golden, J. M. & Graham, G. A. C.**, *Boundary Value Problems in Linear Viscoelasticity*, Springer Verlag, 1988.

[5] **Johnson, C.**, *Numerical Solution of Partial Differential Equations by the Finite Element Method*, Cambridge University Press, 1987.

[6] **Ciarlet, P. G.**, *The Finite Element Method for Elliptic Problems*, Studies in Mathematics and its applications 4, North–Holland, 1978.

[7] **Wheeler, M. F.**, *A-priori $\mathcal{L}_2$ Error Estimates for Galerkin Approximations to Partial Differential Equations*, SIAM J. Numer. Anal. **10** (1973) pp723-759.

[8] **Nečas, J. & Hlaváček, I.**, *Mathematical Theory of Elastic and Elasto–Plastic bodies, an Introduction*, Studies in Applied Mathematics 3, Elsevier Scientific Publishing Company, Amsterdam, 1981.

[9] **Fairweather, G.**, *Finite Element Galerkin Methods for Differential Equations*, Lecture Notes in Pure and Applied Mathematics vol. 34, Marcel Dekker inc., 1978.

[10] **Tricomi, F. G.**, *Integral Equations*, Interscience Publishers, inc., New York, fourth printing 1967.

[11] **Whiteman, J. R., Beagles, A. E. & Warby, M. K.**, *Theoretical and Practical Aspects of Finite Elements in the Context of Some Problems in Solid Mechanincs*, Jber. d. Dt. Math-Verein, **92** (1990) pp 77-88.

[12] **Lees, M.**, *A Priori Estimates for the Solutions of Difference Approximations to Parabolic Partial Differential Equations*, Duke Mathematical Journal, **27** (1960) pp 297-311.

[13] **Linz, P.**, *Analytical and Numerical Methods for Volterra Equations*, Society for Industrial and Applied Mathematics, 1985.

[14] **Wolkenfelt, P. H. M.**, *On the Relation Between the Repetition Factor and Numerical Stability of Direct Quadrature Methods for Second Kind Volterra Integral Equations*, SIAM J. Numer. Anal. **20**, (1983) pp 1049-1061.

[15] **Knauss, W. G. & Emri, I.**, *Volume Change and the Nonlinearly Thermo–Viscoelastic Constitution of Polymers*, Polymer Engineering and Science, **27**, (1987) pp 86-100.

[16] **Schapery, R. A.**, *On Nonlinear Viscoelastic Constitutive Equations for Composite Materials*, Preprint, to appear in: Proceedings of the **VII** International Congress on Experimental Mechanics, Las Vegas, June 8-11, 1992.

[17] **Whiteman, J. R., Shaw, S. & Warby, M. K.**, *Finite Element Methods With Recovery for Problems of Viscoelasticity*, Proceedings of International Conference on Numerical Methods in Engineering and Applied Science, Concepcion, Chile, Nov 1992, to appear.